Rapport

Diarienummer
NV Rapport 2023-12

Projektnummer
Examensarbete, 15 hp

Evaluation of AI-method for measuring and characterizing particles on-line in drinking water treatment

Examensarbete, Högskoleingenjörsexamen Kemiteknik, KTH

Lovisa Ådén
KTH i samarbete med Norrvatten

2023-12-29

DEGREE PROJECT IN CHEMICAL ENGINEERING,
FIRST CYCLE, 15 HP
STOCKHOLM, SWEDEN 2023

Evaluation of AI-method for measuring and characterizing particles on-line in drinking water treatment

LOVISA ÅDÉN

KTH ROYAL INSTITUTE OF TECHNOLOGY
SCHOOL OF ENGINEERING SCIENCES IN CHEMISTRY,
BIOTECHNOLOGY AND HEALTH

DEGREE PROJECT

Bachelor of Science in
Chemical Engineering

Title:	Evaluation of AI-method for measuring and characterizing particles on-line in drinking water treatment
Swedish title:	Utvärdering av AI-metod för att mäta och karaktärisera partiklar on-line i dricksvattenberedning
Keywords:	Turbidimeter, Particle meter, rapid filtration
Work place:	Kommunalförbundet Norrvatten
Supervisor at work place:	Ida Sekizovic
Supervisor at KTH:	Elisabet Brännvall

Student: Lovisa Ådén

Date: 2023-11-02

Examiner: Elisabet Brännvall

Abstract

The municipal association Norrvatten produces drinking water at Görväln WTP for approximately 700,000 residents in 14 member municipalities in the northern Stockholm region. To ensure the drinking water meets quality criteria, the water must be carefully monitored by the WTP.

At Norrvatten there are several rapid filters that remove different types of particles, mainly residues from the previous flocculation step. The running time of the filters can be limited by a filter breakthrough, which means that the filter must be regenerated through backwashing. To detect a filter breakthrough, turbidity measurement is used.

A new advanced AI method, a particle meter, from the manufacturer Uponor is installed at several locations at Görväln WTP. The particle meter is being evaluated as a possible complement to the standard turbidity measurement. The particle meter is a type of advanced image interpretation software that measures and categorizes particles that may indicate disturbances in the drinking water production.

In this project, particle meters placed on-line in three different rapid filtrates were compared with existing on-line turbidity measurements. The aim was to investigate whether the particle meter could detect a filter breakthrough earlier than a turbidimeter and whether the particle meter added any additional valuable information for drinking water production. Data from the period 1 May 2022–30 April 2023 was evaluated in Acurve and Excel.

Periods where filter breakthrough occurred in filters denoted A, B and C were evaluated to see which method indicates a filter breakthrough the fastest. During the studied period, eight filter breakthroughs occurred in filter C (quartz sand), three in filter A (Filtralite NC 0,8-1,6 mm) and none in filter B (Filtralite 70% NC 0,8-1,6 mm and 30% HC 0,5-1 mm. Rapid filter B has a lower flow rate than filter A and C, which contributes to no breakthroughs being found. The particle meter could not detect a filter breakthrough faster than existing turbidimeters. However, total particles correlated with the trend of turbidity between March–June, which could be explained by the higher abundance of B-particles. During the remaining months, turbidity and total particles followed completely different trends. Therefore, the particle meter could potentially be used to detect algal blooms online early during spring, compared to the weekly laboratory analysis of algae. This is also supported by algae in raw water correlating with the trend of B-particles in the rapid filtrate.

Periods where the turbidity was below 0,10 FTU and total particles exceeded 100,000 pcs/ml in filters A, B and C were selected to investigate whether the particle meter provided any additional valuable information. Six events for total particles exceeding 100,000 pcs/ml were found in filter C, two in filter A and none in filter B during the examined period. The lower flow rate as well as the material combination in Filter B could contribute to no events being found. The material in Filter A could also contribute to a lower number of events compared to Filter C. The small particle category, $< 3\ \mu m$, dominated during these periods and is prone to false detections due to fouling of the particle meter. The particle category that correlated with total particles was small particles in filter A and a mixture of B-and F-particles in filter C. B-and F-particles often followed the same trend which could be because particles, mainly algae, have been categorized into both categories at the same time. Events where total particles >100,000 pcs/ml occur means that there are particles in the filtrate periodically which the rapid filters cannot separate, and which are not detected by the turbidimeter. However, these results could be a consequence of false detections.

The particle categorization of the particle meter does not seem to be finished, as only a few of the total particles have been categorized as either B-, C-, F- or small particles. This leads to difficulty in interpreting and using the produced data.

Sammanfattning

Kommunalförbundet Norrvatten producerar dricksvatten på Görvälnverket till ungefär 700 000 invånare i 14 medlemskommuner i norra Stockholmsregionen. För att säkerställa att dricksvattnet uppfyller de kvalitetskriterier som finns måste vattnet noggrant kontrolleras av vattenverket.

Hos Norrvatten finns flertalet snabbfilter som avlägsnar olika typer av partiklar, främst rester från den föregående flockningssteget. Filtrets gångtid kan begränsas av ett filtergenombrott, som leder till att filtret måste regenereras genom backspolning. För att upptäcka ett filtergenombrott används turbiditetsmätning.

En ny avancerad AI-metod, en partikelmätare, från tillverkaren Uponor är installerad på flertalet platser i Görvälnverket. Partikelmätaren utvärderas som ett möjligt komplement till den vanliga turbiditetsmätningen. Partikelmätaren är en typ av avancerat bildtolkningsprogram som mäter och kategoriserar partiklar som kan indikera störningar i dricksvattenberedningen.

I det här arbetet jämfördes partikelmätare placerad on-line i tre olika snabbfiltrat med existerade on-line turbiditetsmätning. Målet var att undersöka om partikelmätaren kunde upptäcka ett filtergenombrott snabbare än en turbidimeter samt om partikelmätaren tillförde någon ytterligare värdefull information för dricksvattenberedningen. Data från perioden 1 maj 2022–30 april 2023 utvärderades i Acurve och Excel.

Perioder där filtergenombrott skett i filter benämnda A, B och C utvärderades för att se vilken mätare som indikerar ett filtergenombrott snabbast. Under den studerade perioden inträffade åtta filtergenombrott i snabbfilter C (kvartssand), tre i snabbfilter A (Filtralite NC 0,8–1,6 mm) och inga i snabbfilter B (Filtralite 70% NC 0,8–1,6 mm och 30% HC 0,5–1 mm. Snabbfilter B har lägre flöde än filter A och C, vilket kan vara en orsak till att inga genombrott hittades. Partikelmätaren kunde inte påvisa ett filtergenombrott snabbare än redan existerande turbidimeter. Däremot korrelerade totala partiklar med trenden för turbiditet mellan mars–juni, vilket kan förklaras av den högre förekomsten av B-partiklar. Under resterande månader följde turbiditet och totala partiklar helt olika trender. Därför skulle partikelmätaren potentiellt kunna användas för att upptäcka algblomningar on-line tidigt under våren, jämfört med de veckovisa laboratorieanalyserna av alger. Detta stöds också av alger i råvatten som korrelerar med trenden av B-partiklar i det samlade snabbfiltratet.

Perioder där turbiditeten var lägre än 0,10 FTU och totala partiklar översteg 100 000 pcs/ml i filter A, B och C valdes ut i syftet att undersöka om partikelmätaren tillförde någon ytterligare värdefull information för dricksvattenberedningen. I den undersökta perioden hittades sex event där totala partiklar översteg 100 000 pcs/ml i filter C, två i filter A och inga i filter B. Den lägre flödeshastigheten samt materialkombinationen i filter B skulle kunna vara orsaken till att inga event hittades. Materialet i filter A skulle också kunna bidra till det lägre antalet event jämfört med filter C. Små partiklar, <3 µm, dominerade under dessa perioder som är en kategori där felavläsningar är vanligt vid fouling av partikelmätaren. Den partikelkategori som korrelerade med totala partiklar var små partiklar i filter A och en blandning av B-och F-partiklar i filter C. B-och F-partiklar följde ofta samma trend vilket skulle kunna bero på att partiklar, främst alger, har blivit indelade i båda kategorierna samtidigt. Att totala partiklar >100 000 pcs/ml förekommer i perioder innebär att det finns partiklar i filtratet periodvis som snabbfiltren inte kan avskilja och som inte detekteras av turbidimetern. Dessa resultat skulle dock kunna vara en konsekvens av feldetektion.

Partikelkategoriseringen hos partikelmätaren verkar inte vara helt färdig hos Norrvatten då endast ett fåtal av de totala partiklarna har blivit kategoriserade som antingen B-, C-, F- eller små partiklar. Detta leder till en svårighet i att tolka och använda framtagna data.

Abbreviations

DAF	Dissolved air flotation
FTU	Formazine turbidity unit
NTU	Nephelometric turbidity unit
WTP	Water treatment plant

Table of Content

1 Introduction

Drinking water must be carefully monitored and meet quality criteria. These criteria include in addition to various microbiological parameters such as turbidity, pH, color and smell [1].

The municipal association Norrvatten produces drinking water for approximately 700,000 people in 14 member municipalities in the northern Stockholm region. The production takes place at the production site Görväln WTP in Järfälla municipality, where the raw water is brought in from Lake Mälaren. The capacity of Görväln WTP is approximately 140 000 cubic metres per day [2].

Multiple purification steps are used in the production of drinking water, including micro-straining, coagulation and flocculation, sedimentation, sand filters, carbon filters, UV reactors, chlorination and pH adjustment [3].

After the coagulation and flocculation steps, the aluminium flocs are sedimented and the water is led to the rapid sand filters. In these filters residues of the flocs that have not settled in the previous sedimentation basins as well as suspended matter such as fibres, mud, sludge, parasites, viruses, bacteria, and algae are removed [4]. Rapid filters remove particles larger than the voids, but also smaller particles through adsorption and sedimentation [4].

Over time, particles accumulate in the filter and a filter skin builds up which gives an increasing filter resistance. When the resistance reaches the range of approximately 1–2 meter water column, the filter must be backwashed [4]. The filter's running time, the time between two backwashes, can also be limited by a filter breakthrough. Backwashing the filters costs both water and time because production is at a standstill, therefore it is important to carefully monitor when a filter breakthrough occurs.

To detect a filter breakthrough early, the turbidity of the filtrate is measured [4]. Turbidity measurement is an optical method and a measure of particle content, which can be used to measure drinking water quality [5]. An increase in turbidity indicates that there is a reduced separation of microorganisms [4].

A new advanced AI method, a particle meter from Uponor, is installed at several locations in Görväln WTP as a possible future complement to the turbidimeters. Three of these particle meters are in the rapid filters. The particle meter has a type of advanced image interpretation software that measures and characterizes particles that may indicate disturbances in the drinking water preparation.

In purpose of detecting a filter breakthrough as early as possible, the particle meter must be evaluated and compared with existing turbidimeter. Of interest for the comparison is whether the AI method is more sensitive, for example produces a faster result, and easier can detect a filter breakthrough. The examined filters in this project are rapid filters denoted A, B and C.

The methods for solving the problem have been literature studies and interpretation of data from the particle meter and turbidimeter in Acurve and Excel. The data used in the evaluation was from 1 May 2022 – 30 April 2023. By choosing a yearlong interval, seasonal variations could be studied.

1.1 Aim, Objective, and Research Questions

The evaluation aims to answer the question of whether the particle meter provides additional, and for drinking water preparation, valuable information compared to already existing turbidimeter.

To limit the work, certain periods of time between 1 May 2022 – 30 April 2023 will be selected for the study. The selection of periods depends on if an interesting event occurs, such as a filter breakthrough.

Following research questions are used to reach the objective:

- Can the particle meter placed in rapid sand filtrate detect a filter breakthrough faster than already existing turbidimeter?

- Does the particle meter placed in rapid sand filtrate provide any additional, valuable information for the drinking water production than already existing turbidimeter?

2 Theoretical background

The chapter provides an overview of relevant background necessary for the evaluation. The topics covered are the principles of drinking water treatment, rapid filters, the turbidimeter and particle meter.

2.1 Drinking water production at Görväln WTP

The drinking water production plant Görväln WTP uses multiple different processes to provide clean drinking water to their member municipalities. The steps included are micro-straining, coagulation, flocculation, sand filtration, carbon filtration, UV treatment, chlorination, and pH-adjustment.

The first purification step is micro-straining which is used to separate algae and fish among others [3]. After micro-straining, the water is led through a pumping station and on to the coagulation step, where suspended and colloidal particles are removed. The coagulation occurs in a mixing chute where the coagulation chemical aluminum sulphate is added to the water [3]. The next step is a flocculation chamber where the aluminum sulphate form flocs [3].

The surface of suspended and colloidal particles naturally has a negative charge, which causes them to repel each other. The reason a positive ion is added as a coagulation chemical, such as Al^{3+}, is to neutralize the negatively charged colloidal and suspended particles. When the surface of the colloidal and suspended particles is neutralized, the van der Waals forces can act and flocs starts to form [6]. The flocs become even larger by addition of the flocculation aid sodium silicate. The aluminum flocs attract other suspended and colloidal particles like microorganisms, mud, and decomposed plant parts [3].

The flocs are separated through sedimentation in the following sedimentation basins. The separation is based on differences in density. The flocs will sink to the bottom of the basins where they will be removed by a large scraper [6]. Dissolved air flotation, DAF, has been built into the pre-existing sedimentation basins. DAF is a more effective separation technique and can help with increasing capacity of the WTP if necessary, but it requires more energy than sedimentation [7].

Thereafter the water is led to the sand filters that mechanically separates residues of the aluminium flocs, colloidal and suspended particles by letting water pass through a bed of sand [4].

To remove odour and taste, the water passes through beds with granulated carbon. Next, the water goes on to the UV-reactors that inactivate bacteria and viruses, and monochloramine is added to prevent bacterial growth in the pipelines. Before sending the water to a reservoir, such as water towers, the water is pH-adjusted to reduce corrosion that may occur in the pipes [3].

2.2 Rapid filtration

Rapid filtration is a common type of filtration and a term for filters that have a high filtration rate [8]. Rapid filters usually have a filtration rate in the range of $5 - 10 \frac{m^3}{m^2 \cdot h}$ [4]. Because of the high filtration rate, they do not require a large area [8].

The filter bed is usually around one meter deep but depending on different parameters such as desired flow rate and turbidity of incoming water, the bed can be made deeper. The filter media can consist of one or multiple mediums, materials. The filter medium should be inert, and not affect the water. The filter medium used at Norrvatten WTP is quartz sand, which is a common material used for rapid filtration in drinking water treatment [4].

Rapid filters come as open or closed filters. The rapid filters at Görväln WTP are open filters. Open rapid filters utilize gravity and have the water coming from above and going downwards through the filter. A common form of open rapid filters are rectangular tanks made from concrete. The pressure drop over the filter bed is compensated through having a certain height of water above the filter bed, usually in the range of 0,3-3 m of water column [8].

Rapid filters separate particles larger than the voids between the particles of the filter medium. Smaller particles are also separated through adsorption and sedimentation. Among the separated particles are residues of the flocs that have not settled in the previous sedimentation basins and suspended matter in the form of fibres, mud, sludge, parasites, viruses, bacteria, and algae. Which sizes of particles that can be separated depends on the filter material, the finer the material, the better particle separation. Since a fine-grained material has a better separation ability, the filter needs to be backwashed more often [4].

The bottom of the filter is constructed to hinder the filter material from escaping, thus only giving passage for water. The design of the filter bottom also helps to evenly distribute water over the filter during backwashing and filtration [4].

Over time, the filter starts to become saturated with particles and a filter cake builds up on top of the filter bed. The more saturated the filter becomes, the larger the filter resistance (measured in meter water column) becomes. The filter's running time is commonly around 1-7 days and can be limited by a too high filter resistance or filter breakthrough [4]. When the filter resistance becomes too high, or measured turbidity of the filtrate reaches a certain limit, the filter needs to be regenerated through backwashing [4]. At Norrvatten, the filters are backwashed after set time intervals.

During the backwashing of Norrvatten's rapid filters, the water flow is coming from the filter bottom going upwards. The particles removed from the filter will rise to the top where the turbid water is drained from the tank through gutters. Important parameters for backwashing are rate and distribution of water over the filter. Without a good distribution of water during backwashing, parts of the filter could become blocked. The filtrate during the first 15-30 minutes after a backwashing process is called a first filtrate and is often drained from the filter because of its high turbidity [4].

The rapid filter has a filtration cycle, illustrated in Figure 1, which is the time between two backwashes [4]. The diagram shows the resistance as a function of time. Where the resistance drops drastically in the diagram is where the backwashing process is performed. After the filter has been backwashed, the resistance builds up linearly until the next backwash is started.

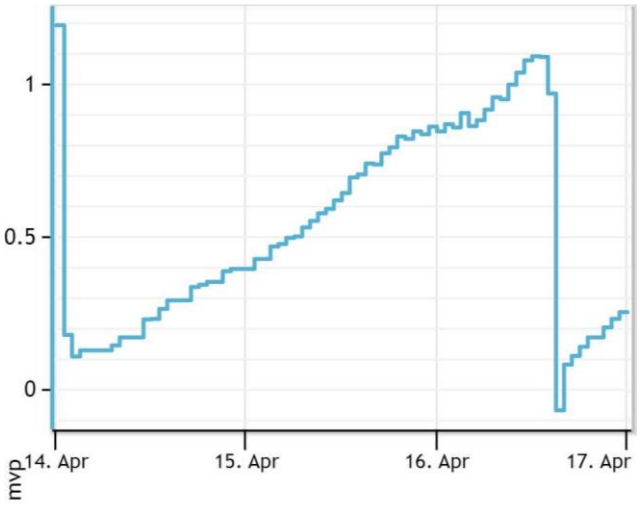

Figure 1. Resistance [mvp] in rapid filter A at Görväln WTP between April 14th-17th 2023.

2.2.1 Filter materials

The studied rapid filters at Görväln WTP, denoted A, B and C, consist of different materials. Rapid filter C uses quartz sand as filter medium whereas the filter medium used in rapid filter A and B is a material called *Filtralite* [9].

Rapid filter A uses the Filtralite material called NC 0,8-1,6 mm. Rapid filter B contains of 70 % NC 0,8-1,6 mm and 30% HC 0,5-1 mm [9]. NC is a low density clay-aggregate and HC is a high density clay-aggregate [10]. The use of Filtralite materials in filter A and B is an attempt to increase the hydraulic capacity of the rapid filters, and specifically for filter B an increased quality of the filtrate [9].

2.3 Turbidity measurement

Turbidity can be described as cloudiness or decrease in transparency [11]. The principle of turbidity measurement is based on scattering of light made by suspended and colloidal particles in the water [12].

The instrument used for measuring turbidity is called a turbidimeter [11]. The turbidimeter transmits light with initial beam intensity I_0 through a sample, where the suspended particles will scatter light as they get hit by the light beam. The change of transmitted light intensity is measured and results in a value of turbidity [11]. The suspended or colloidal particles that scatter light are normally in the size range of $\mu m - nm$ [12].

The relationship between beam intensity and initial beam intensity when measuring turbidity, is described by Equation 1. Where I represent the resulting outgoing beam intensity and I_0 represent the initial beam intensity. The τ is the turbidity coefficient and l is the length of the medium [12].

$$I = I_0 e^{-\tau l} \quad (1)$$

The reliability of turbidity measurement is low at very high and low turbidities. In drinking water, the turbidity is normally low, and if the difference in light intensity is small it can be difficult to detect. Factors that can influence the measured turbidity value is, for example, particle size and color. When particles have different shapes and colors, the light will be scattered and absorbed differently, even when the medium contains the same amount of particles in milligrams per liter [11].

The turbidimeters are placed on-line in each sand filtrate. The turbidimeter model in rapid filter A and B is the Micro TOL from HF scientific, inc. The model of turbidimeter used in rapid filter C is Hach 1720E Low Range Turbidimeter. Both turbidimeters have the same accuracy of ± 0.02 NTU or ±2%, depending on which one is greater, under 40 NTU [13] [14]. NTU, nephelometric turbidity unit, is a turbidity unit and is equivalent to FTU, formazine turbidity unit, which is used in the evaluation. The difference between the units is the method used for turbidity measurement.

The reporting limit for turbidity at Görväln WTP is 0,10 FNU based on the accredited analysis measurement range which is between 0,1-200 FNU [15].

2.4 Particle meter

The particle meters used at Görväln WTP are of the model Qumo from the manufacturer Uponor. One of these are placed on-line in each of the examined rapid filtrates.

The particle meter classifies particles by size and shape by creating a holographic image with laser light. Total number of particles is calculated by an image processing algorithm. The algorithm calculates a statistical average for total number of particles every three minutes by capturing and processing the particles [16].

When categorizing incoming particles, they are compared to a large set of size and shape classes that are created by the AI's algorithm, which are visualized by *water fingerprint diagrams*. An incoming particle's fingerprint is compared to a reference fingerprint and the difference is calculated and visualized [16].

The particle meter can also measure physical parameters such as temperature, electric conductivity, and turbidity equivalent [17].

The particle meter is placed after the turbidimeter, and same stream of water goes through both instruments. Therefore, a delay is to be expected for the particle meter compared to the turbidimeter.

2.4.1 Particle categories

The particle meter has around 300 internal categories that have been condensed to four broad categories, small, B-, F- and C-particles. (E-mail E Hämäläinen 2023-06-27). The particles are categorized based on size, and symmetry or asymmetry [16].

The category small particles include particles smaller than 3 micrometers. According to Esa Hämäläinen, development manager at Uponor, the detection efficiency decreases below 2 micrometers. When fouling occurs on the particle meter, the small particle category is susceptible to false detections (E-mail E Hämäläinen 2023-06-27).

B-particles consists of multiple different organic and inorganic suspended particles with complex shapes [16]. B-particles are usually larger than a few micrometers [18]. B-particles are common in natural waters and include, for example algae, protozoa, flocs, organic debris, sand, and grit. Although the particles are common in natural waters, they are rare in purified drinking water. If the B-particle concentration is higher than usual it could indicate a disruption of water quality, for example the water source. Number of B-particles could also show contamination in the water source, which is shown with a heightened value during a longer period [16].

F-particles include fiber-shaped particles and are commonly found in wastewater and stormwater. The fiber-shaped particles originate from sources like food, toilet paper and

plants [16]. However, the F-particles also seem to register some species of algae according to Uponor (E-mail E Hämäläinen 2023-06-27).

C-particles are normally found in wastewater and stormwater [18]. The C-particles could have complex shapes and are often in the size range of tens of micrometers. The C-particle category could indicate external material getting into the water system (E-mail E Hämäläinen 2023-06-27).

In addition to the four broad particle categories, the particle meter has a Total particle count which is an indication of the total amount of solid particles and a sum of all detected particles [16].

2.5 Factors affecting particle content

Several factors can affect the particle content in water as well as the turbidimeter and particle meter readings.

2.5.1 Seasonal variations

There are different classes of lakes, and Lake Mälaren is a dimitic lake which is a cold temperate lake. Dimitic lakes stratify in both summer and winter, which means that the lake water is divided into layers that do not mix properly. The layers are created because of different physical and chemical properties, where the most notable difference is the water temperature [19].

When fall comes around, the surface water is cooled down and the density is increased which causes it to sink. With help from the wind the water is circulated and eventually the whole lake is consistent in temperature, this is called fall circulation [20]. In springtime, the surface water starts heating up and the water temperature becomes consistent throughout the water body. Just like the fall circulation, the water is circulated because of wind and currents [20].

Another important phenomenon is the algal bloom that occurs during the warmer part of the year. Except for the summer algal bloom, there is a large spring bloom and a smaller fall bloom. The spring and fall algal bloom mainly consist of diatoms that are non-toxic [21].

2.5.2 Disturbances in measuring instruments

When the turbidimeter is being calibrated, the on-line turbidity measurements may show different values during the calibration time (Personal communication Ida Sekizovic 5 May 2023). The particle meter is mechanically cleaned automatically. It may happen that the cleaning does not work for some reason, which leads to the accumulation of particles in the meter. This is shown in the data as particle values that are constantly increasing (Personal communication Ida Sekizovic 29 May 2023).

3 Methodology

The chapter provides information on how the study was conducted. The program used to collect data for the evaluation was Acurve. The data from Acurve was downloaded and processed in Microsoft Excel.

3.1 Filter breakthrough

The focus of the study was whether the particle meter could detect a filter breakthrough earlier than the turbidimeter.

The studied periods were selected based on when filter breakthroughs were detected, defined as when the turbidity exceeded 0,15 FTU. The periods around the peaks in turbidity were carefully studied to observe if either the particle meter or turbidimeter indicate a filter breakthrough sooner than the other. A high turbidity can also indicate a backwashing process, and complimentary data of flow rate and resistance was used to rule out these events. Exactly where the filter breakthrough occurred was determined as the first value over 0,15 FTU. How long the filter had been running when the filter breakthrough occurred was also noted.

How many particles per milliliter that indicate a filter breakthrough was unknown. Norrvatten does not have a set internal limit yet because the instrument is still under evaluation. Therefore, it was determined for each filter breakthrough individually where particles per milliliter increased significantly. Additional obtained information was the dominating particle category, where the total particles increased significantly and the particle category that best followed the trend of total particles. The information was obtained to determine possible connections between particle category and filter breakthrough.

3.2 Drastic increase in amount of particles

To determine if the particle meter provided any additional and valuable information for the drinking water production compared to already existing turbidimeter, periods when the particle meter indicates an event of some sort were selected. The periods of interest were decided to when total particles exceeded 100 000 [pcs/ml].

To conclude if a certain particle was more abundant, the different categories of particles were compared and visualized in separate diagrams with B-particles, C-particles, F-particles, and small particles. Which particle trend that best followed the total particles was noted, as well as the dominating particle category in numbers.

3.3 Seasonal variations

The seasonal variations were also considered due to the possibility of the particle meter working differently depending on the season. Several diagrams were plotted to show these seasonal variations. One diagram was plotted to show how algae varied with temperature throughout the year. Algae was also compared with the turbidity values of the raw water. Another diagram was plotted to compare the trends of algae in raw water and B-particles in the sand filtrate. Moreover, B-particles and total particles were compared to see what proportion of the total particles are made up of B-particles. Raw water temperature and different parameters from the particle meter were on-line values., however, the algae and turbidity values of the raw water were weekly since they were derived from the weekly analyses at Norrvatten's laboratory.

4 Results and discussion

Results from the data evaluation will be presented along with additional data valuable for the evaluation such as seasonal variations of the water's particle content.

4.1 Filter breakthroughs

During the period of May 2022 – April 2023, several turbidity breakthroughs occurred, where the turbidity exceeded 0,15 FTU, in rapid filter A and C. No filter breakthroughs were found in rapid filter B. Note that some breakthroughs might not have been included due to not being found because of the large amount of data at hand.

4.1.1 Filter breakthroughs in rapid filter A

In this section, all filter breakthroughs found in filter A are presented. The filter breakthroughs found in rapid filter A, as well as complimentary information, are presented in Table 1. Rapid filter A consists of Filtralite NC 0,8-1,6 mm.

Table 1. Filter breakthroughs in rapid filter A (consisting of Filtralite NC 0,8-1,6 mm) during the period of May 2022 – April 2023.

Filter break-through	Reaction turbidimeter	Turbidity [FTU]	Reaction particle meter	Total particles [pcs/ml]	Dominating particle category	Running time at break-through [h]
A.1	2022-06-28 08:15	0,17	2022-06-28 08:17	5 166	Small particles	6
A.2	2022-10-24 15:01	0,15	2022-10-24 15:12	4812	Small particles	44
A.3	2022-10-27 04:54	0,18	not clear	-	Small particles	21

Turbidity and total particles in rapid filter A for breakthrough A.1 on June 28th, 2022, are shown in Figure 2. The flow rate and filter resistance for A.1 are presented in Figure 3. The type of particles occurring during filter breakthrough A.1 are visualized in Figure 4.

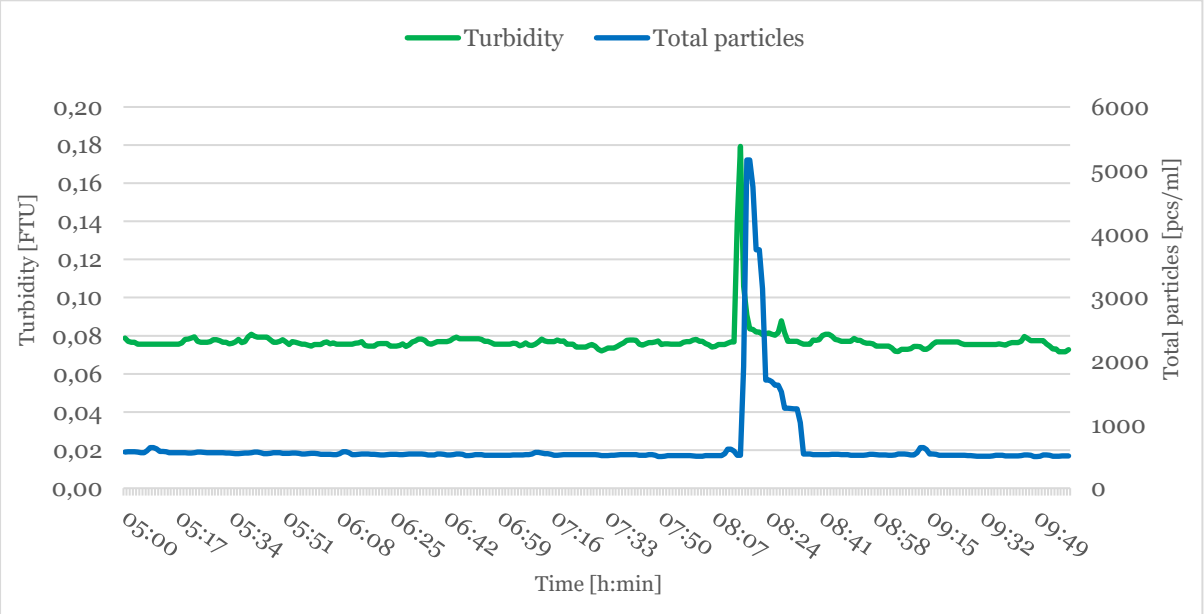

Figure 2. Turbidity and total particles during filter breakthrough A.1.

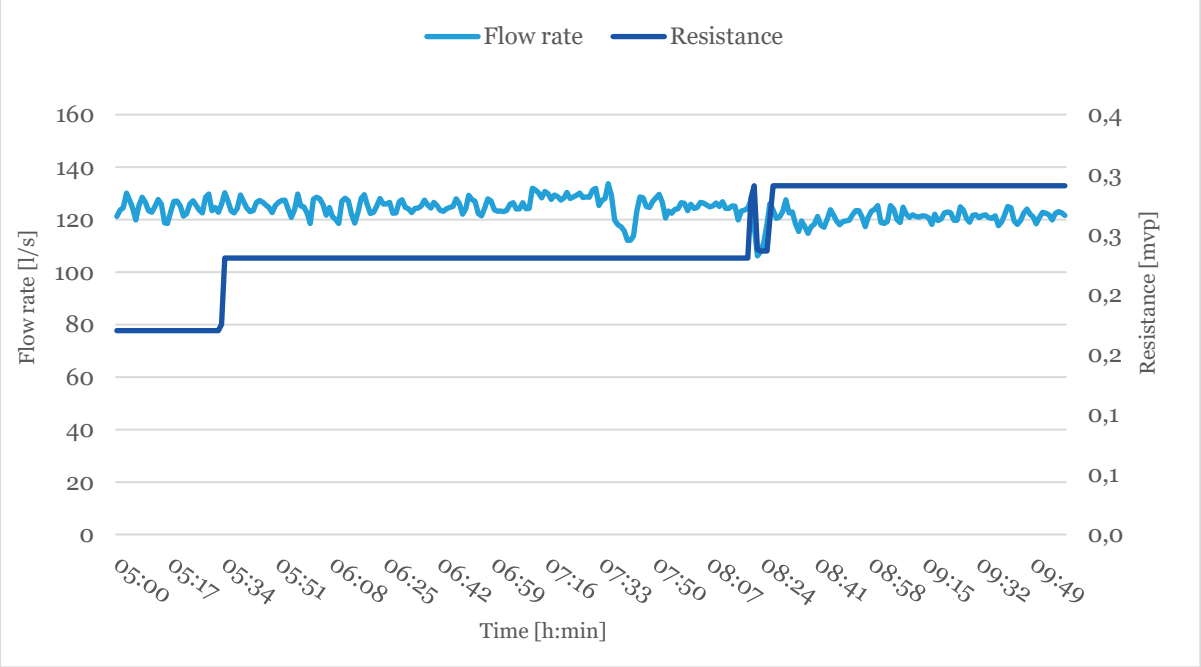

Figure 3. Flow rate and resistance during filter breakthrough A.1.

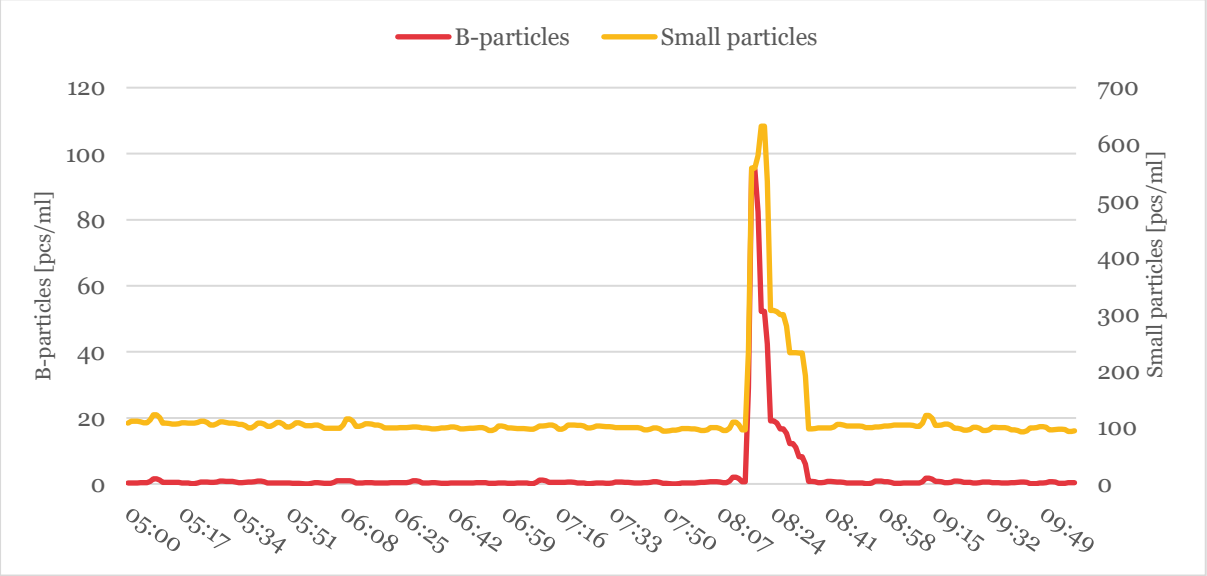

Figure 4. B-particles and small particles during filter breakthrough A.1.

The turbidity and total particles peak at approximately the same time, as seen in Figure 2. The same stream of water goes through both the particle meter and the turbidimeter. First through turbidimeter and then through particle. A few minutes difference between the reaction of the turbidimeter and the particle meter is therefore negligible.

The slowly increasing and nearly constant flow rate ensures that there is no back wash or other event that causes the turbidity and particles to increase. Breakthrough A.1 occurred after only 6 hours of running time since the last backwash. The short running time could mean that the backwashing process was insufficient which contributed to more particles than normal coming through the filter.

The dominating particle category was small particles, and B-particles. C- and F-particles were negligible due to occurring in very low numbers, or possibly not detected by the particle meter. Even though small particles are the dominating particle category by quantity, total particles in Figure 2 most closely correlate to the trend of B-particles in Figure 4.

The trends of turbidity and total particles during filter breakthrough A.2 is shown in Figure 5. The flow rate and filter resistance for A.2 are presented in Figure 6. The type of particles occurring during filter breakthrough A.2 are visualized in Figure 7 and 8.

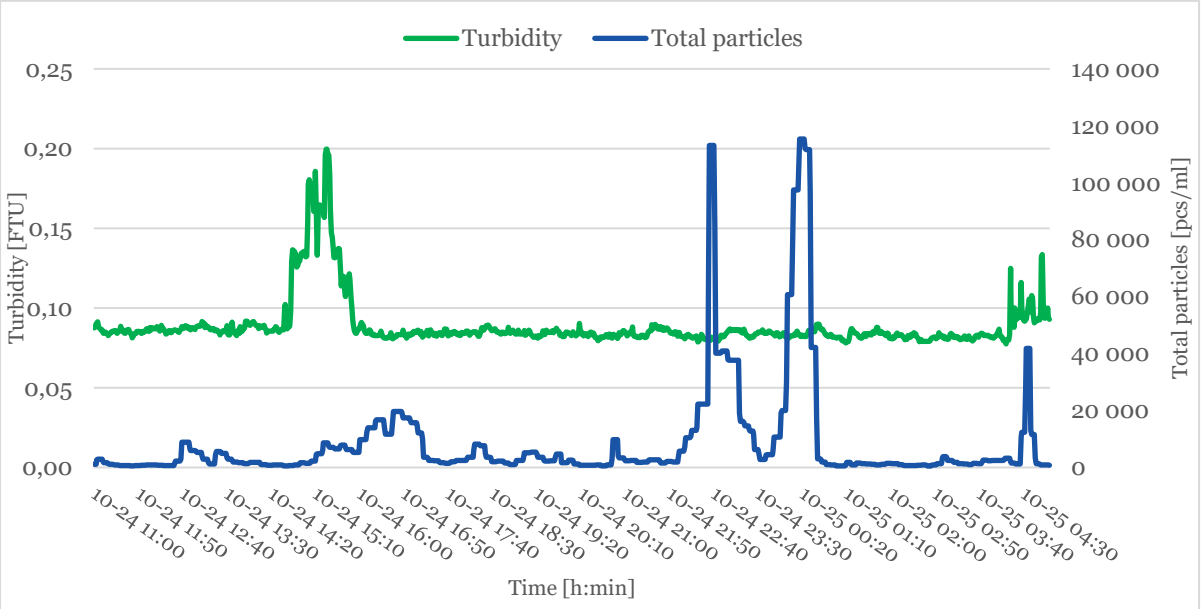

Figure 5. Turbidity and total particles during filter breakthrough A.2.

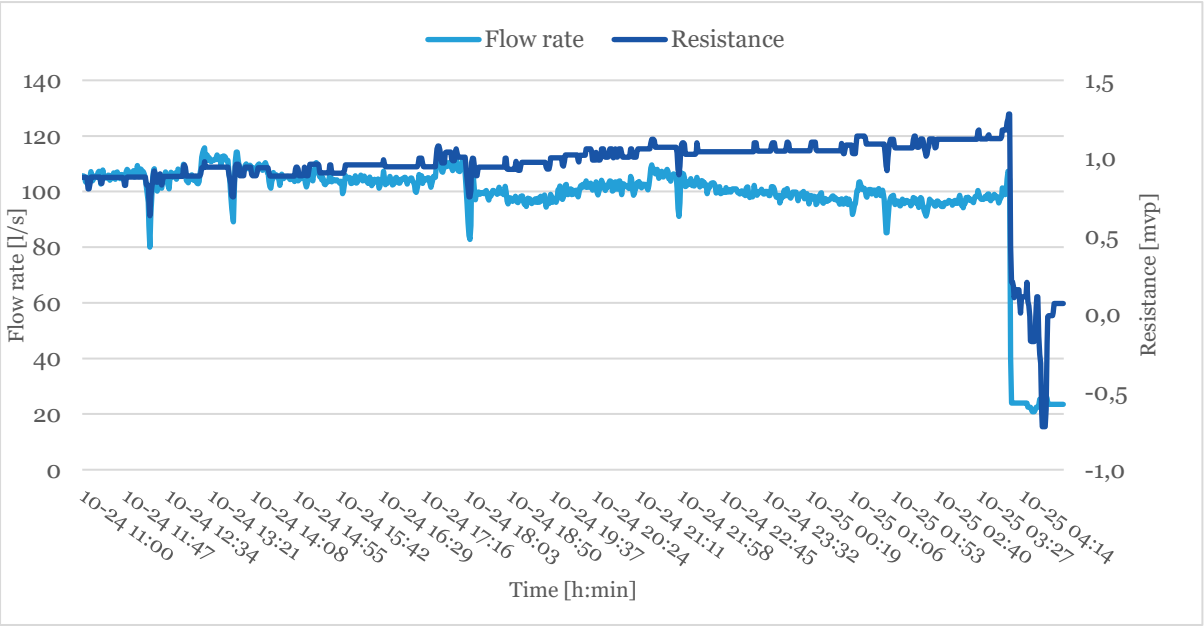

Figure 6. Flow rate and resistance during filter breakthrough A.2.

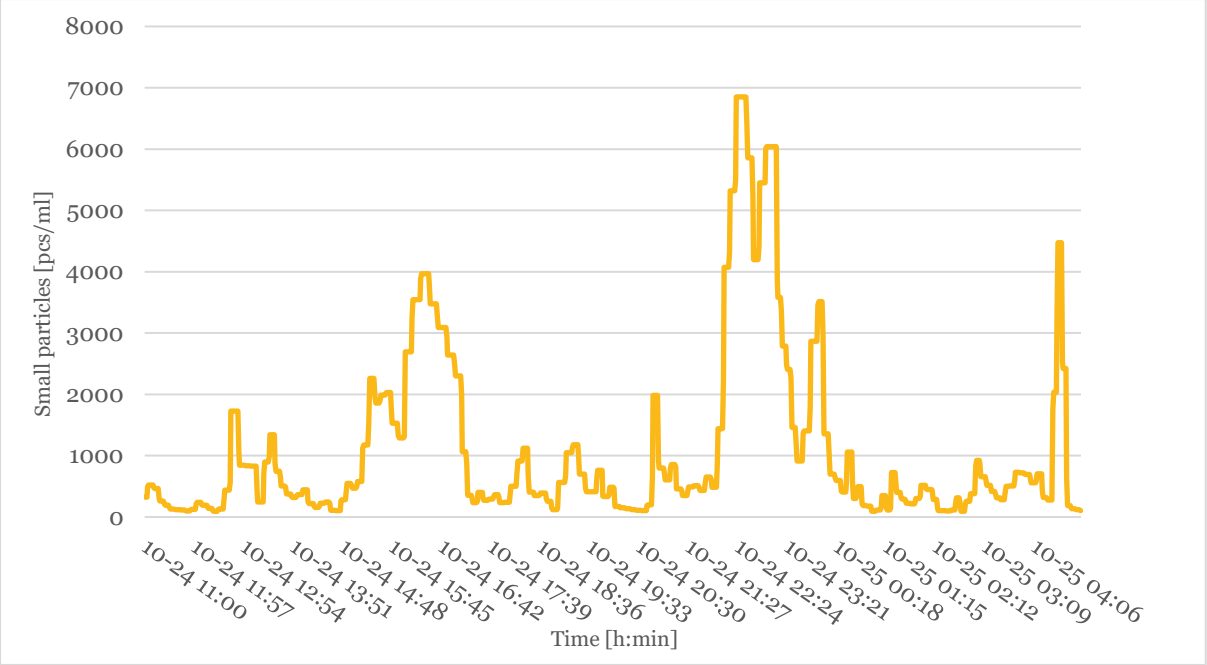

Figure 7. Small particles during filter breakthrough A.2.

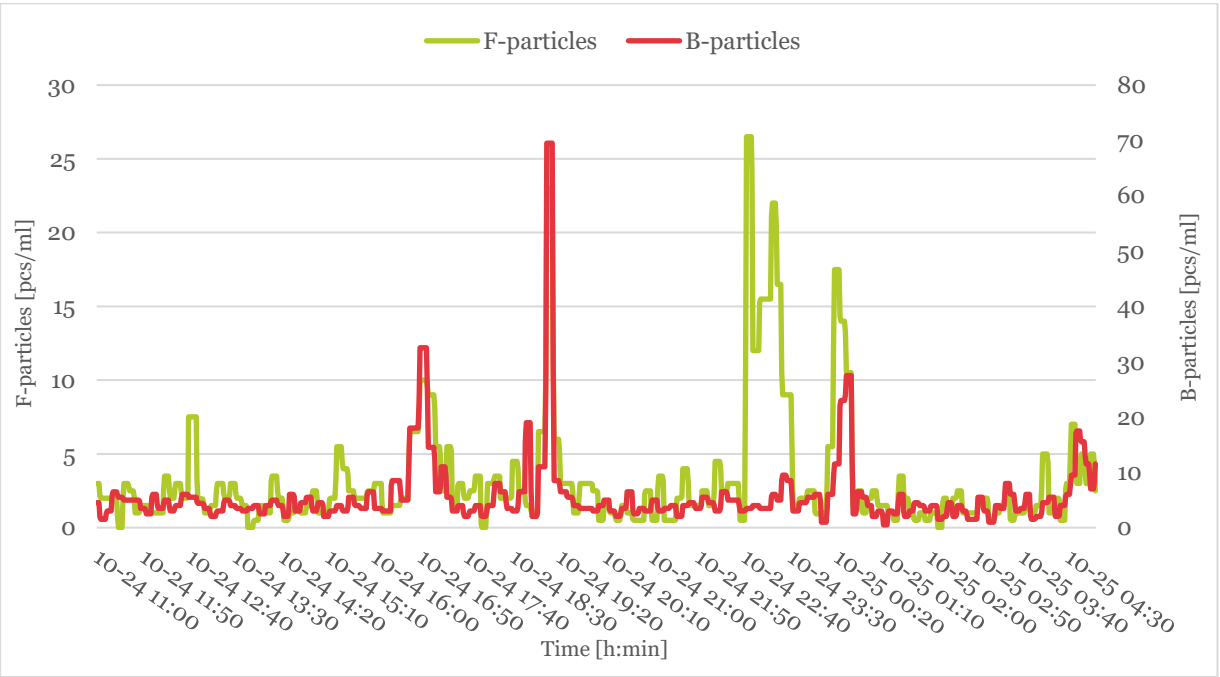

Figure 8. F-particles and B-particles during filter breakthrough A.2.

The turbidimeter reacts approximately eleven minutes before the particle meter. It is not clear whether the small peak in total particles is a reaction at all on the filter breakthrough. The flow rate and resistance in Figure 6 confirms that the turbidity and total particles are not a response to a backwashing process.

Moreover, the particle meter clearly registers some event multiple hours later. The event could be an indicator of a particle breakthrough. The filter breakthrough and the particle meter's reaction are most likely not related, but it is interesting that the turbidimeter registers an event that the particle meter does not (or perhaps very little), and the particle meter registers an event that the turbidimeter does not.

According to the particle meters categorization, the dominating particle during period A.2, both during the turbidity peak and total particles peak, is small particles. The trend for small particles is shown in Figure 7, and B-and F-particles can be seen in Figure 8. B-and F-particles occurred in lower quantities than small particles, and do not seem to follow the trend of total particles for the most part. However, during the drastic increase in total particles, F-particles also increases along with small particles.

Filter breakthrough A.3, seen in Figure 9, occurred on the 27th of October 2022. Flow rate and resistance for breakthrough A.3 is shown in Figure 10. The dominating particle category during this event was small particles, which is shown in Figure 11. Other particles that occurred during the same period are shown in Figure 12.

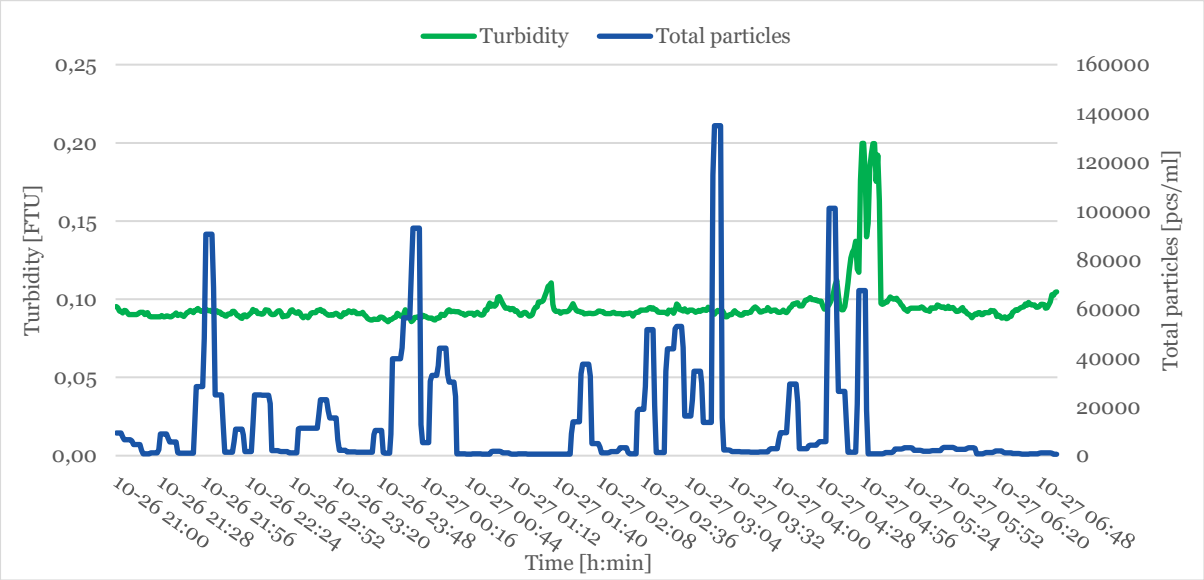

Figure 9. Turbidity and total particles during filter breakthrough A.3.

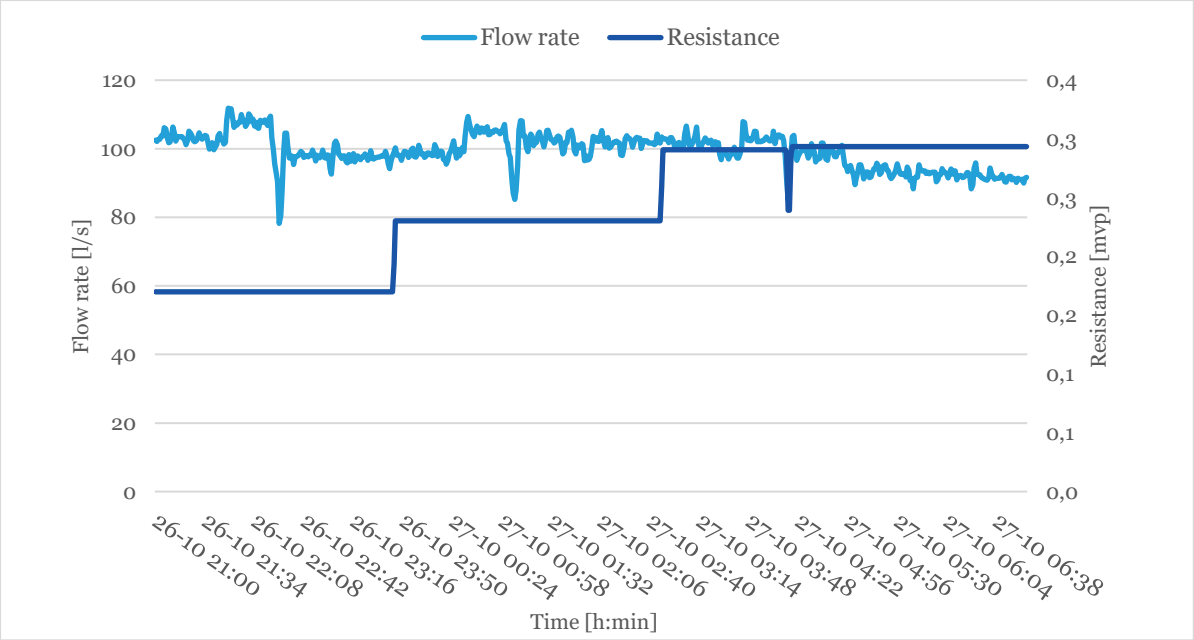

Figure 10. Flow rate and resistance A.3.

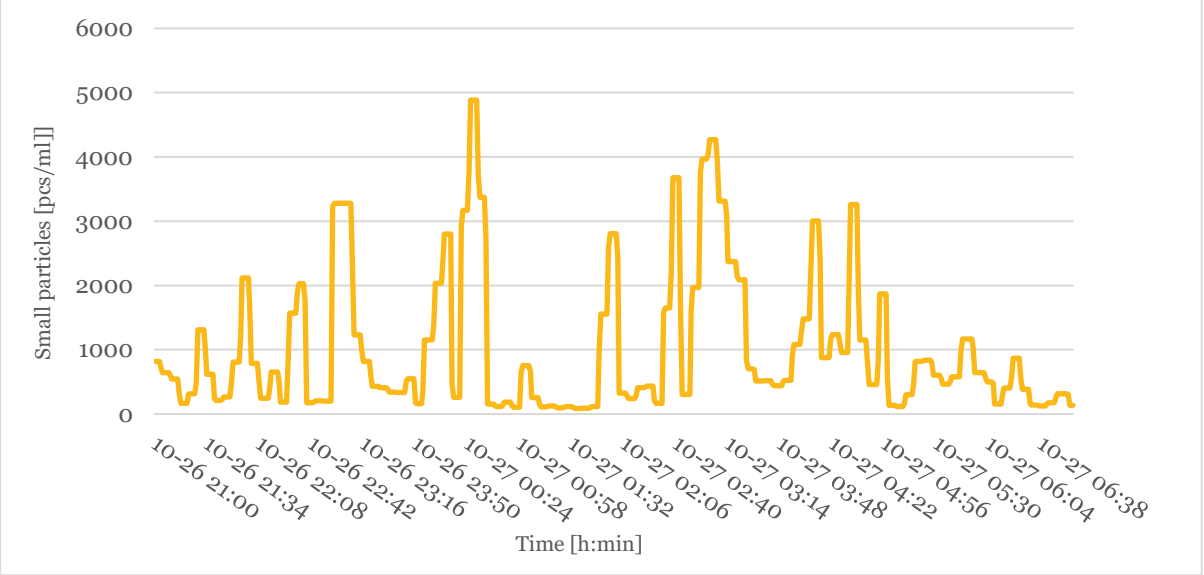

Figure 11. Small particles A.3.

The trend of small particles in Figure 11 does not follow the trend of total particles in Figure 9 perfectly, but they are very similar. B- and F-particles are shown in Figure 12; however, their trends do not follow the same trend as total particles.

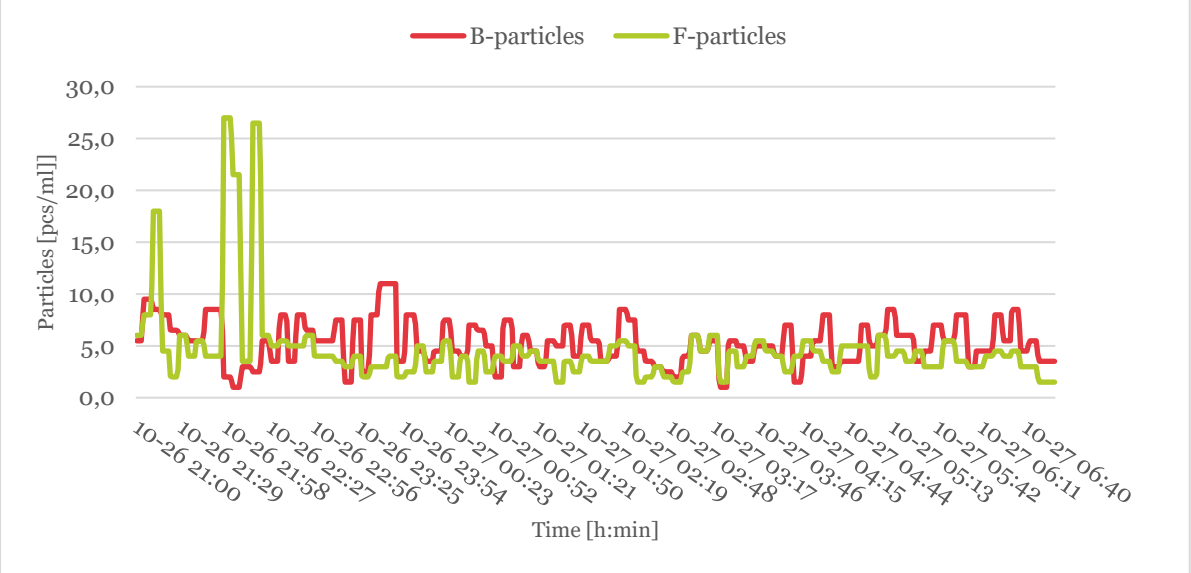

Figure 12. B-particles and F-particles during A.3.

The particle meter's reaction differs from previous breakthroughs A.1 and A.2. The particle meter shows a volatile trend before the turbidity peaks at 04:54. The turbidimeter do not seem to notice the large amount of particles in the filtrate before the filter breakthrough. Turbidity and particles do not correlate in this case, and a higher turbidity does not correspond to a higher number of particles. The high number of particles shown from 21:00 to the turbidity peak at 04:54 are not due to an increased flow rate or resistance.

The three different breakthroughs look different in all three cases, A.1-A.3. During filter breakthrough A.1, the difference between the particle meters and turbidimeters reaction is clearly visualized and interpreted. Whereas A.2 and A.3 are more difficult to interpret due to the turbidimeter and particle meter following different trends. Breakthrough A.1 occurred in June and A.2 and A.3 in October. The reason for the trend of total particles, turbidity, B-particles, and small particles follow the same trend. The particle meter seems to correlate to the turbidimeter when larger particles, such as B-particles which include algae, are present in the water.

The three events have different running times, as seen in Table 1. A.1 has only 6 hours of running time which could indicate an insufficient backwash. Filter breakthrough A.2 has the longest running time, 44 hours, out of the three and A.3 has 21 hours of running time. There does not seem to be a trend between these three breakthroughs related to running time.

The particle that occurred in the highest amounts in all three cases are small particles. Because the turbidimeter and particle meter generally are not following the same trend, it could mean that the turbidimeter has difficulty registering the small particles.

4.1.2 Filter breakthroughs in rapid filter C

The filter breakthroughs in rapid filter C based on turbidity exceeding 0,15 FTU are presented in Table 2. Event C.1, C.2, C.3 and C.5 are presented in this section and event C.4, C.6, C.7 and C.8 are presented in Appendix I.

Table 2. Filter breakthroughs in rapid filter C during the period of May 2022 – April 2023.

Filter breakthrough	Reaction turbidimeter	Turbidity [FTU]	Reaction particle meter	Total particles [pcs/ml]	Dominating particle category	Running time at filter breakthrough [h]
C.1	2022-05-18 12:57	0,15	2022-05-18 13:02	39 304	B-particles	55
C.2	2022-09-14 17:37	0,15	Not clear	-	Small particles	60
C.3	2022-09-14 19:55	0,15	Not clear	-	Small particles	62
C.4	2022-09-20 02:04	0,15	Not clear	-	Small particles	60
C.5	2022-10-29 17:57	0,16	Not clear	-	Small particles	59
C.6	2023-03-10 09:48	0,20	2023-03-10 09:48	34 021	Small particles	58
C.7	2023-04-04 13:13	0,20	2023-04-04 13:17	42 173	B-particles	47
C.8	2023-04-05 01:47	0,15	2023-04-04 01:48	27 496	Small particles	59

The turbidity and total particles during filter breakthrough C.1 are shown in Figure 13. Figure 14 shows the flow rate and filter resistance during the period. B-particles and small particles during event C.1 is shown in Figure 15.

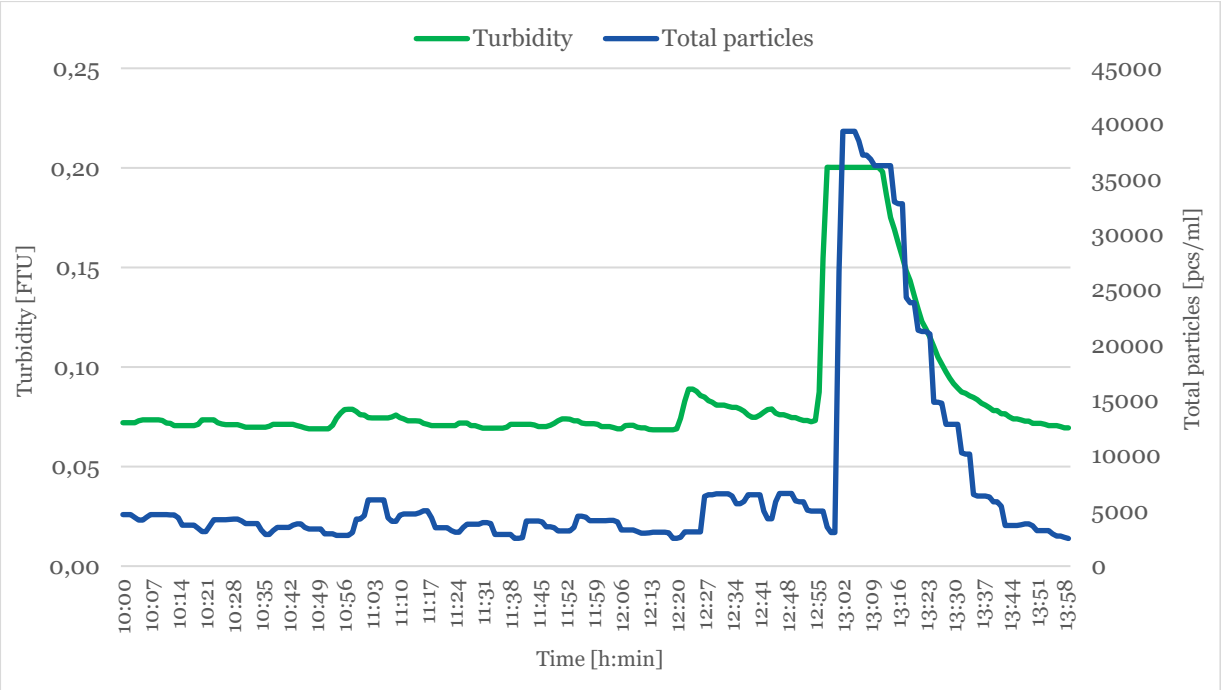

Figure 13. Turbidity and total particles in C.1.

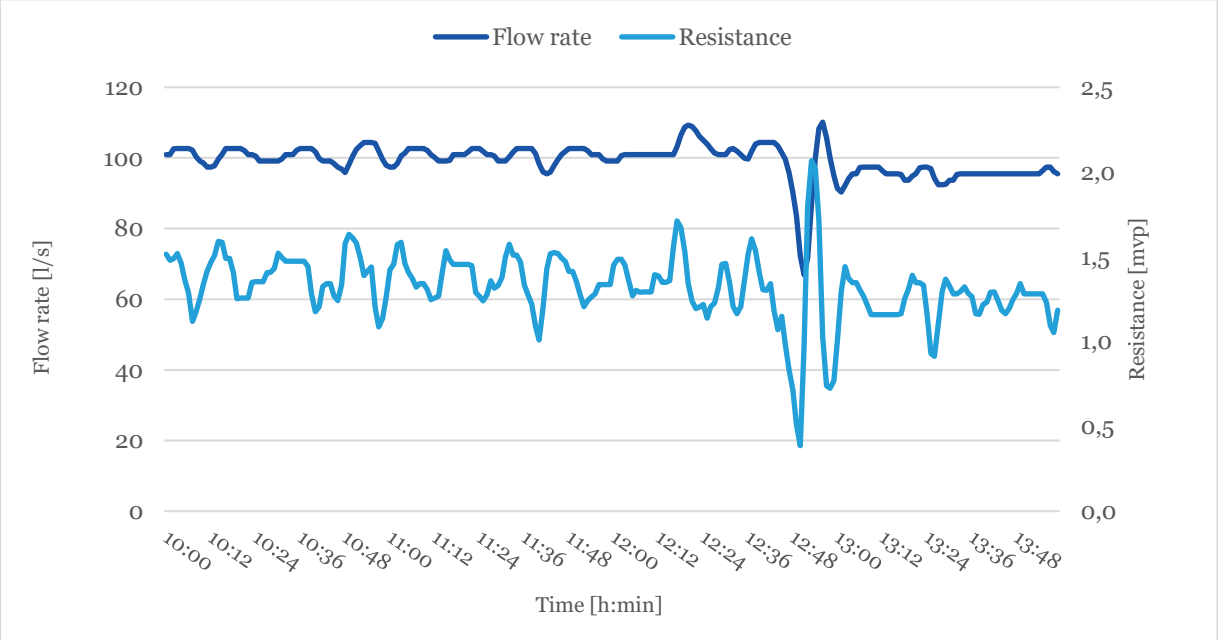

Figure 14. Flow rate and resistance C.1

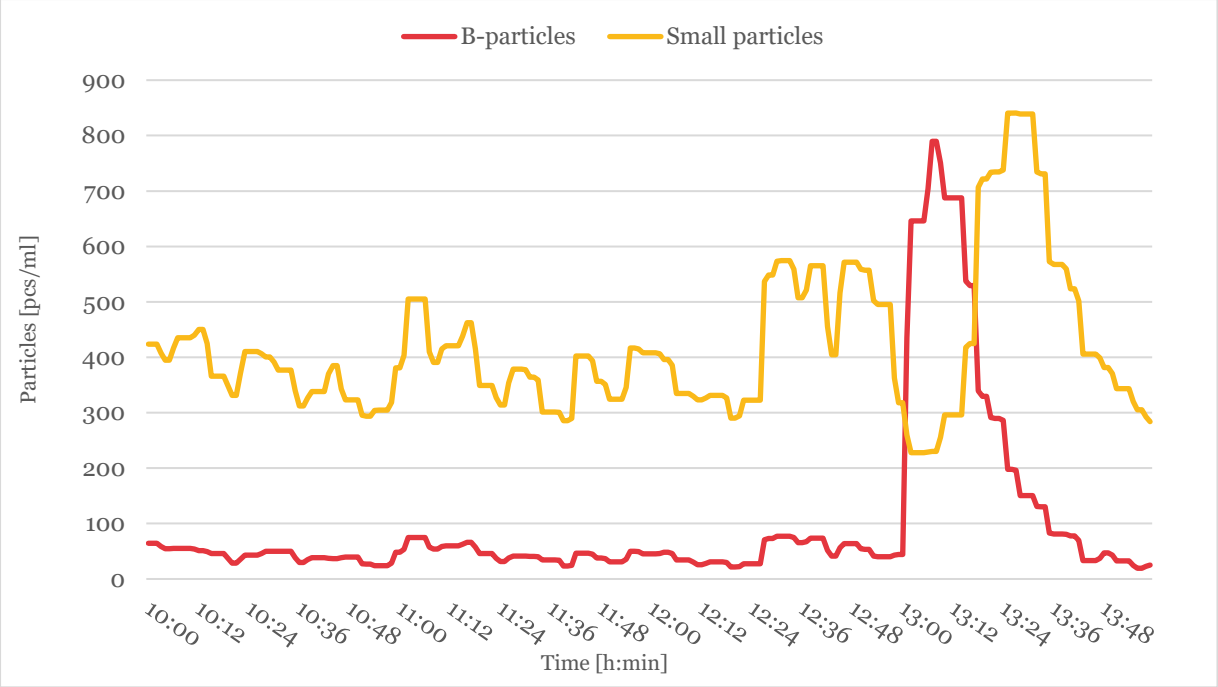

Figure 15. B-particles and small particles C.1.

Filter breakthrough C.1 in Figure 13 show a negligible difference between the particle meter and turbidimeter's reaction. The decrease in flow rate and resistance could be the cause of the heightened turbidity, however, it is not a backwashing process.

Small particles occur in higher concentrations than B-particles during the entire event C.1, but at 13:02 the B-particles rapidly increase. The trend of B-particles correlates with the trend of total particles in Figure 13. The trend of total particles also correlates with the turbidity, but with a delayed reaction. Since filter breakthrough C.1 happens in the month of May, it seems correct that there are higher concentrations of B-particles which include algae.

Figure 16 shows two breakthroughs where the first, C.2, starts at 17:37, and the second, C.3, starts at 19:55. Breakthrough C.2, however, appear to happen because of the increased flow rate, which can be seen in Figure 17, which also increases turbidity. When the flow rate is lowered, the turbidity decreases. In between the turbidity peaks, a peak in total particles occur. The trends of turbidity and total particles do not correlate.

The turbidity and total particles during filter breakthrough C.2 and C.3 are shown in Figure 16. Figure 17 shows the flow rate and filter resistance during event C.2 and C.3. B-particles and small particles during event C.2 and C.3 are shown in Figure 18.

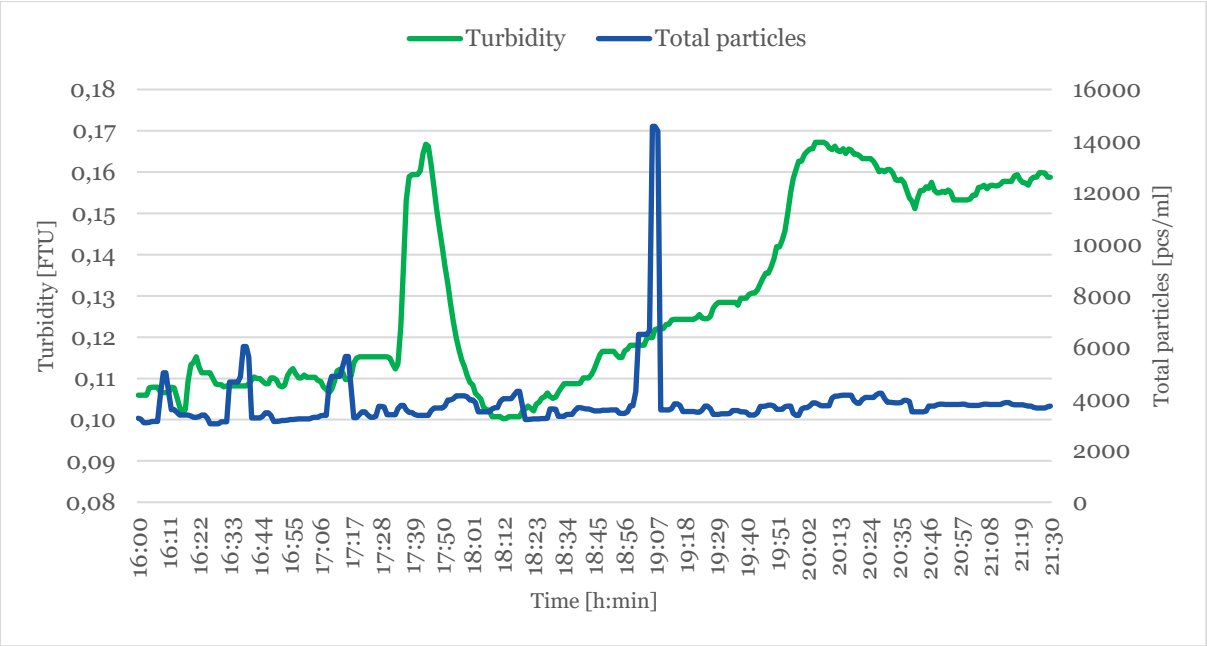

Figure 16. Turbidity and total particles during C.2 and C.3.

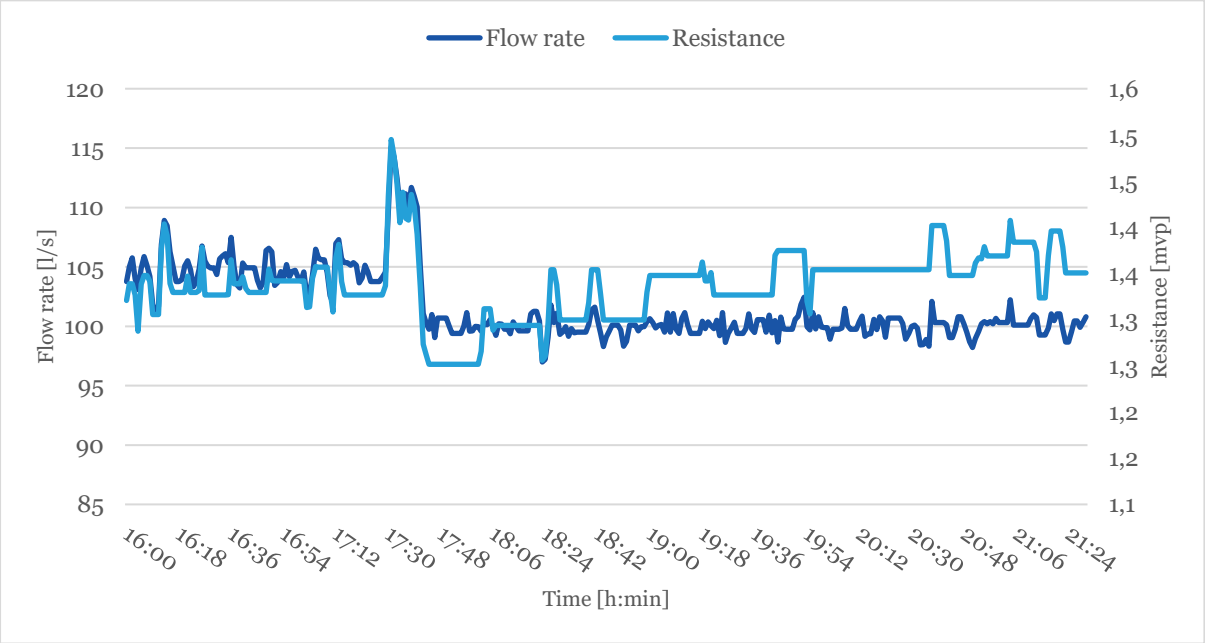

Figure 17. Flow rate and resistance C.2 and C.3.

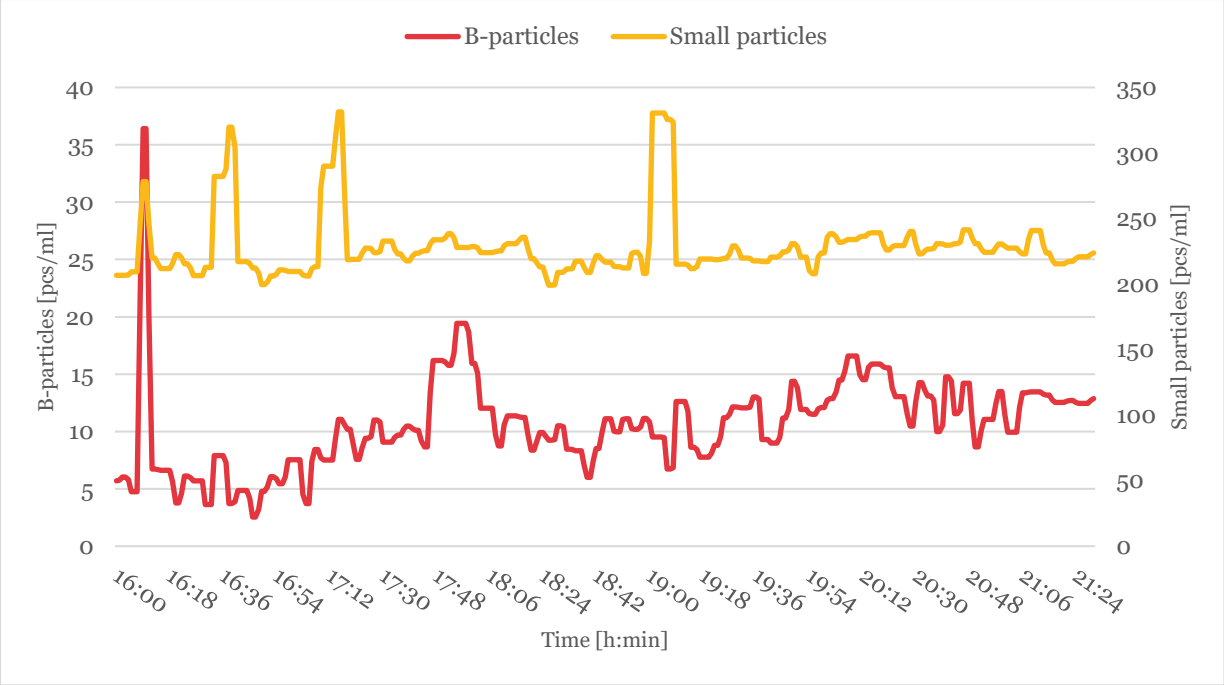

Figure 18. B-particles and small particles during even C.2 and C.3.

Event C.2, which is the first turbidity peak in Figure 16 could be a reaction to the increased flow rate and resistance which can be seen in Figure 17. However, the second turbidity peak, which reaches >0,15 FTU at 19:55, is not a result of an increase in flow rate or resistance.

Small particles follow approximately the same trend as total particles and increases around the time where total particles increase. On the other hand, B-particles show an increase around the time where the first filter breakthrough, C.2, occurs. B-particles seem to follow the whole turbidity trend better than total particles, but not perfectly. Filter breakthrough C.3 is caused a steady upgoing trend of turbidity and happens 62 hours after a backwash, which most likely means that the filter has become saturated, and it is time for a new backwash.

Turbidity and total particles are around breakthrough C.5 are shown in Figure 19. Flow rate and resistance during event C.5 are shown in Figure 20. Small particles and B-particles during event C.5 are visualized in Figure 21.

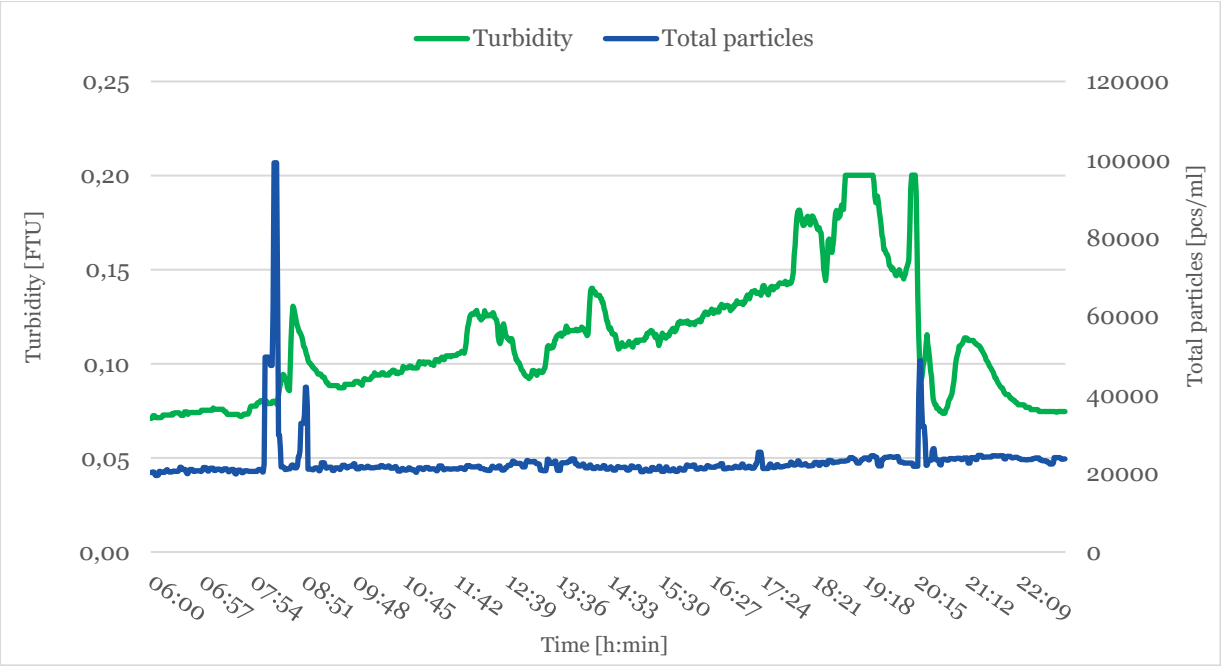

Figure 19. Turbidity and total particles in C.5.

Figure 20. Flow rate and resistance in C.5.

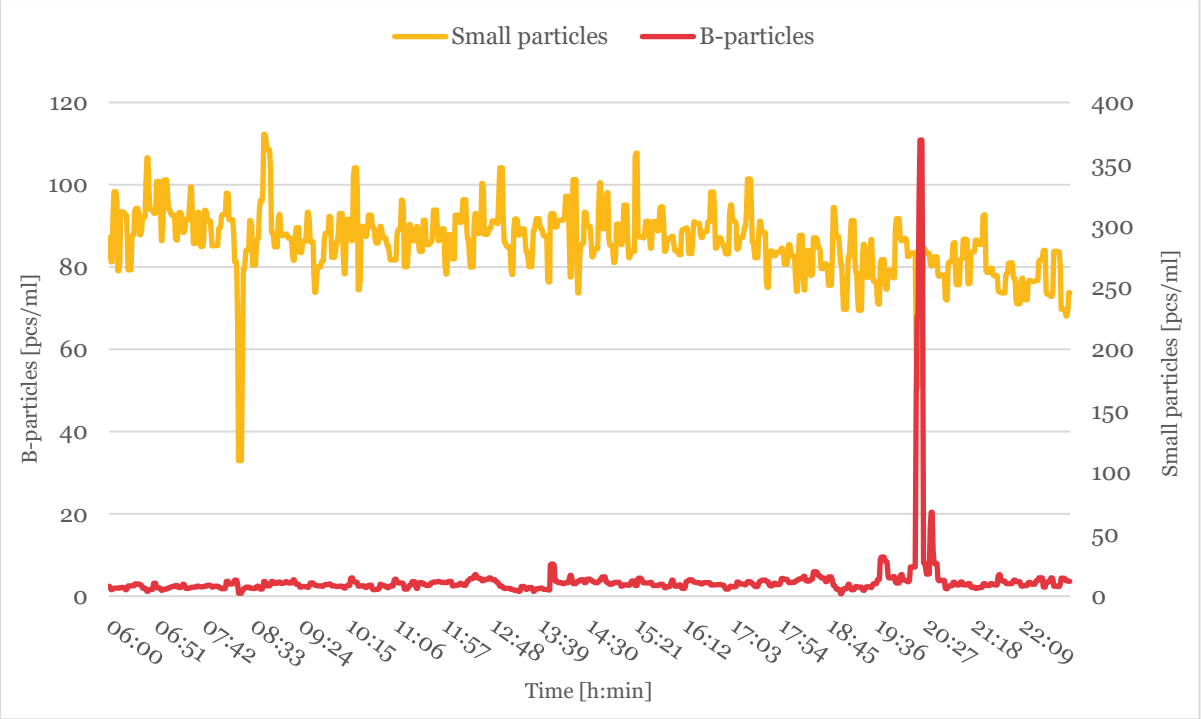

Figure 21. B-particles and small particles in C.5.

The particle meter registers a high number of total particles in the beginning of the period and a peak in turbidity occurs right after, although it is <0,15 FTU and does not qualify as a breakthrough. The peak of total particles could possibly be a result of an automatic cleaning of the instrument. After the small turbidity peak, the turbidity shows an upgoing trend until a breakthrough occurs at 17:57. Total particles correlate to the trend of turbidity.

Neither the trend of small particles or B-particles seem to correlate with either turbidity or total particles, which can be seen in Figure 21. However, when total particles peak around 08:00, small particles decrease.

The decrease in small particles may be a misleading result as it may be a false detection caused by fouling or other particles contributing to an incorrect result. At the point of turbidity breakthrough, the filter had been running for 59 hours, which means the filter probably has become saturated.

4.1.3 Main findings

Filter breakthrough C.4, C.6, C.7 and C.8 are presented in Appendix I. In some cases, the turbidity breakthrough and total particles peak occur at different times (C.4, C.7 and C.8), while at filter breakthrough C.6, the turbidimeter and particle meter react at approximately the same time and approximately follow the same trend. In all cases, B-particles best seem to correlate with the trend of total particles.

In summary, which method has the fastest reaction is not clear. The turbidimeter reacts clearly before the particle meter in four out of eleven cases in total. Filter breakthrough A.2 is unclear whether the reaction of the particle meter is strong enough to be included. In some cases, the particle meter registers activity several hours before the turbidimeter. This is most likely not a reaction to the same activity, but the particle breakthrough could be an indicator of an ongoing event with more particles than usual that will contribute to a shorter running time of the filter, however, this would need more evaluation.

No specific difference can be noticed between filter A and C with respect to which instrument reacts first. More data would need to be studied, especially since only three breakthroughs were evaluated in filter A.

In A.1 and A.2 the turbidity meter reacts first. In the third studied breakthrough, A.3, in rapid filter A, it is unclear if the particle meter shows any reaction due to the long period of elevated values of total particles that may have occurred due to false detections or fouling.

In rapid filter C, the turbidimeter clearly reacts before the particle meter in three cases, and at the same time in one case. In four cases it is difficult to interpret if the turbidity and total particle peaks are reactions to the same event, therefore the particle meter's reaction is marked as Not clear.

In most studied filter breakthroughs, the particle that dominated according to the particle meter was small particles. In two cases, B-particles were the dominating category, C.1 and C.7. In some cases, B-particles contributed strongly to the trend of total particles.

The studied breakthroughs were mainly from spring and fall, and there is a difference on how well the particle meter and turbidimeter follow the same trend. During breakthrough A.1, C.1, C.6, C.7 and C.8, the particle meter follow the same trend as the turbidimeter and reacts at the same time or a few minutes after. The common denominator is that they occur during the months of March, April, May, and June, where B-particles occur in higher concentrations, which is consistent with the algal bloom occurring during this period. The B-particle trends are the ones that correlate the best with both turbidity and total particles in these cases. The particle meter seems to work best during these months in terms of particle categorization.

The particle meter data is more difficult to interpret during the fall months of September and October where breakthroughs A.2, A.3, C.2, C.3, C.4, and C.5 occur. The trends of the particle meter and turbidimeter do not correlate as well, and the type of particle that dominates is small particles.

Data from the particle meter is at times misleading because the categorization does not seem to be completely ready. The number of total particles in most cases much higher than the total of B-, C-, F- and small particles.

In filter A, the running time at filter breakthrough varied between 6-44 hours and in filter C it varied between 47-62 hours. The running time is higher among the breakthroughs in filter C, which means the filters most likely have been saturated which in turn is the cause for filter breakthroughs.

The materials in the filters are different. Filter B, where no breakthroughs were found, consists of both NC 0,8-1,6 mm and HC 0,5-1 mm which means it has an even finer material than filter A. The material could be a reason that no breakthroughs were found. Additionally, rapid filter B has a lower flow rate due to the smaller grain size and shorter running time because of a faster increasing filter resistance.

Filter C consists of quartz sand and filter A of NC 0,8-1,6 mm. The NC-material has a lower porosity than quartz sand, has a better separation and can handle a higher flow rate. The better separation in filter A could be the reason so few filter breakthroughs were found compared to filter C.

4.2 Drastic increase in number of particles

In this section multiple events where the particle meter has registered an event and not the turbidimeter are presented. The events were selected based on the criteria that total particles

show values > 100 000 [pcs/ml] sometime during the period. No events were found in filter B.

4.2.1 Drastic increase in number of particles in rapid filter A

Drastic increases of particles found in rapid filter A are presented in Table 3.

Table 3. Periods where drastic increases of particles were found in rapid filter A consisting of Filtralite NC 0,8-1,6 mm.

Event	Period	Dominating particle type	Particle type that best follows total particles
A.4	2022-11-06 06:00 - 2022-11-07 21:00	Small particles	Small particles
A.5	2022-04-24 00:00 - 2022-04-30 23:59	Small particles	Small particles

Turbidity and total particles during event A.4 are shown in Figure 22 and the filter resistance and flow rate are shown in Figure 23. The best correlating particle type during event A.4 is shown in Figure 24.

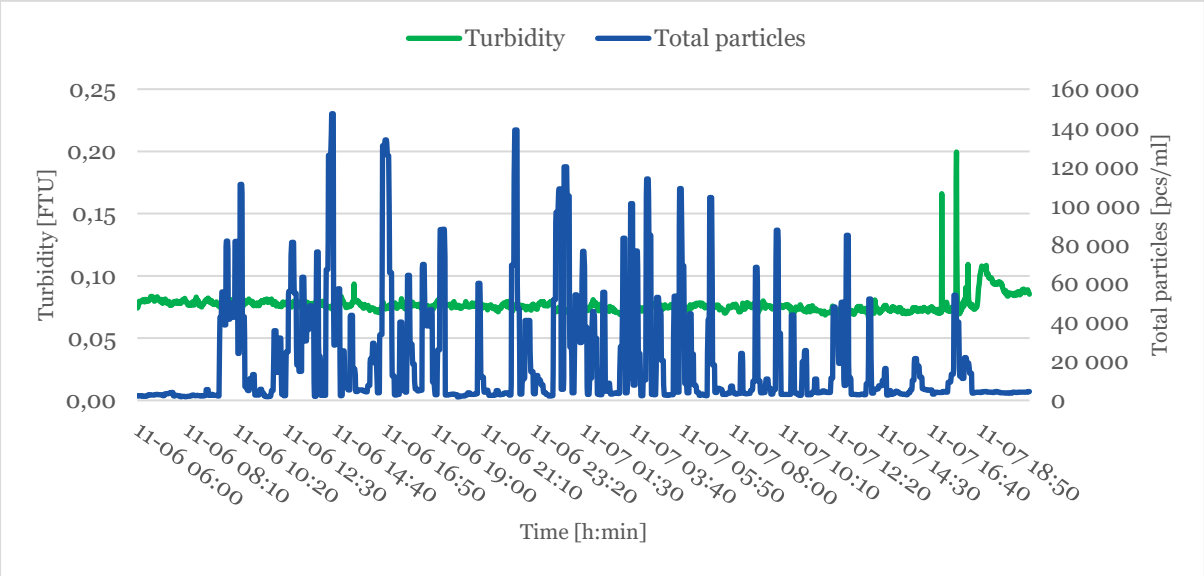

Figure 22. Total particles and turbidity during event A.4.

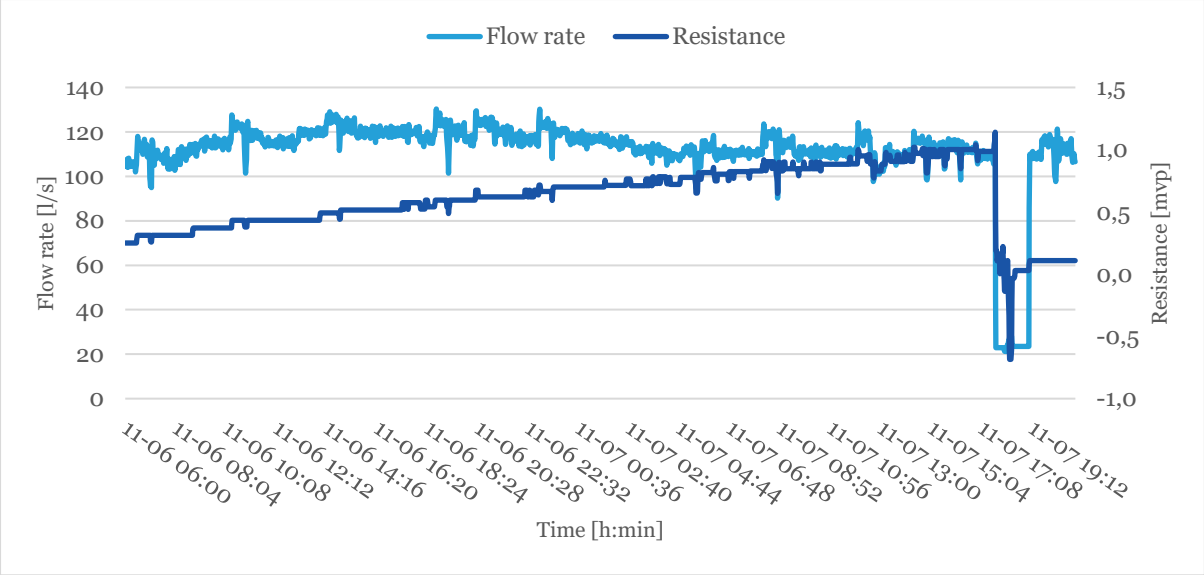

Figure 23. Flow rate and resistance during event A.4.

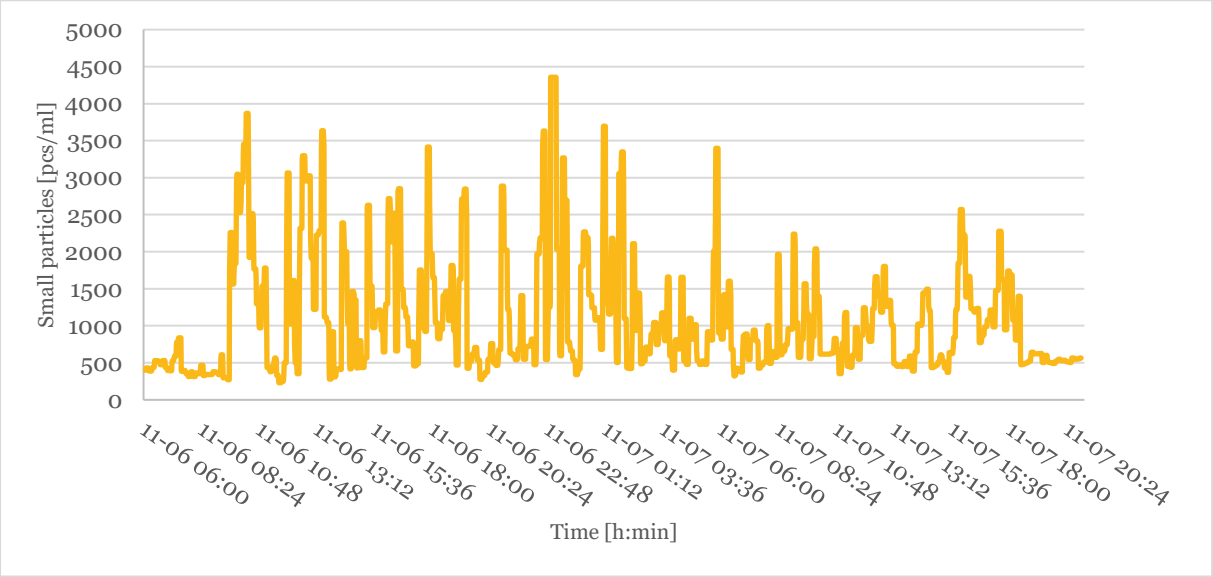

Figure 24. Small particles during event A.4.

The total particles show high activity reaching >140 000 [pcs/ml]. The turbidity is steadily <0,1 FTU. The high turbidity values occur at the end of the period because of a backwashing process, which is confirmed by the flow rate and resistance in Figure 23. The turbidimeter do not seem to register small particles. Small particles dominate during the period and reaches values > 4000 [pcs/ml].

Event A.5 covers a longer period, April 24th – 30th. The turbidity and total particles are shown in Figure 25. The flow rate and filter resistance are shown in Figure 26. Small particles during event A.5 are shown in Figure 27 and B-particles are shown in Figure 28.

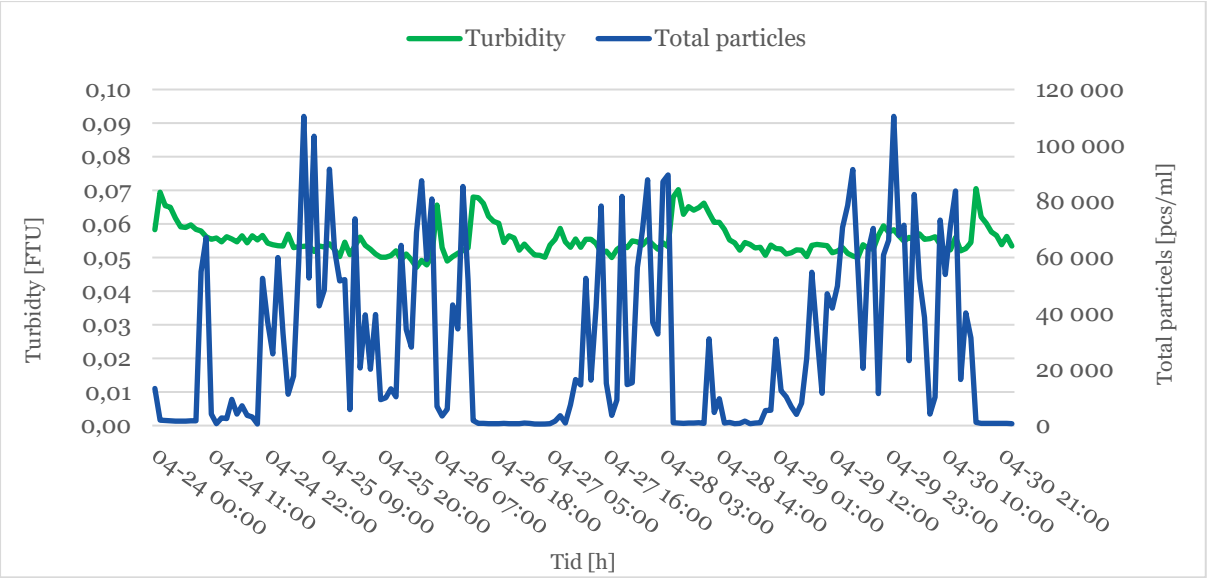

Figure 25. Turbidty and total particles during event A.5, values per hour.

Figure 26. Flow rate and resistance during event A.5.

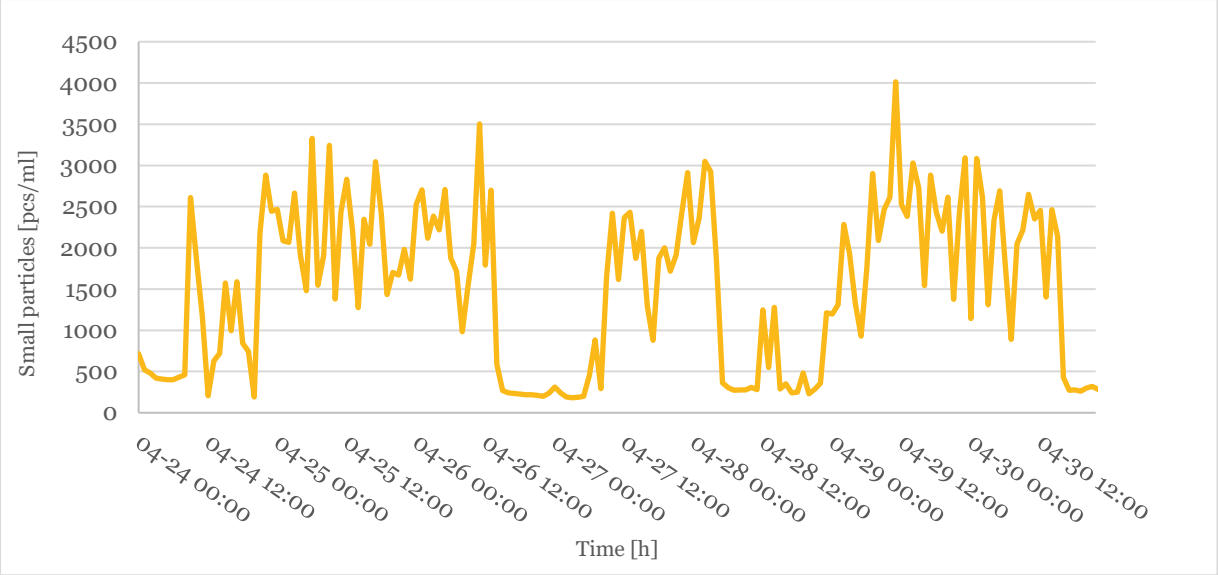

Figure 27. Small particles during event A.5.

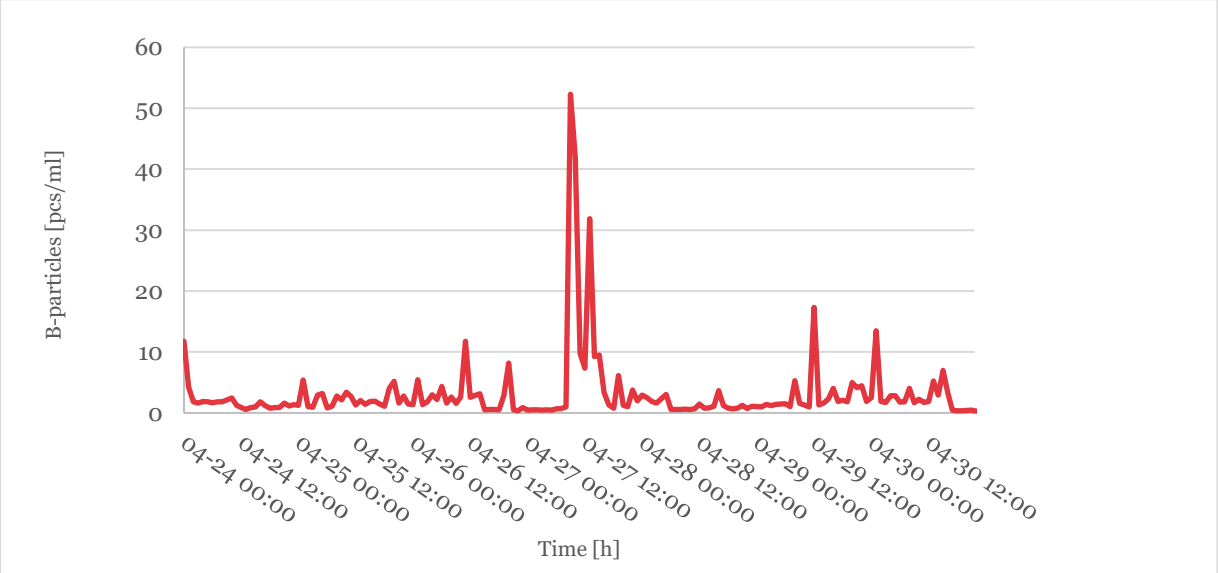

Figure 28. B- particles during event A.5.

Total particles show high values reaching >100 000 [pcs/ml] and the turbidity is < 0,1 FTU for the whole period, see Figure 25. Multiple backwashing processes occur during the period, which can be seen in Figure 26.

The trend of small particles correlates with total particles and is also the dominating particle category during the period. The particle category that occurs in second highest values is B-particles, however the particle category follows a different trend and do not correlate with either total particles or turbidity.

4.2.2 Drastic increase in number of particles in rapid filter C

Drastic increases of particles found in filter C are presented in Table 4. Event C.9 and C.14 are discussed in this section. Event C.10 to C.13 are presented in Appendix II.

Table 4. Drastic increases of particles found in filter C.

Event	Period	Dominating particle type	Particle type that best follows total particles
C.9	2022-10-08 07:00 - 2022-10-11 23:59	Small particles	B-particles and F-particles
C.10	2022-10-31 12:00 - 2022-11-13 23:59	Small particles	B-particles and F-particles
C.11	2022-11-25 00:00 - 2022-11-26 12:00	Small particles	B-particles
C.12	2022-12-09 00:00 - 2022-12-12 12:00	Small particles	B-particles
C.13	2022-12-17 00:00 - 2022-12-20 19:00	Small particles	B-particles and F-particles
C.14	2023-04-16 00:00 - 2023-04-26 14:00	Small particles	F-particles

Event C.9 covers the period October 8th– October 11th. The turbidity and total particles are shown in Figure 29. The flow rate and filter resistance are shown in Figure 30. B-particles and F-particles during event C.9 are shown in Figure 31 and small particles are shown in Figure 32.

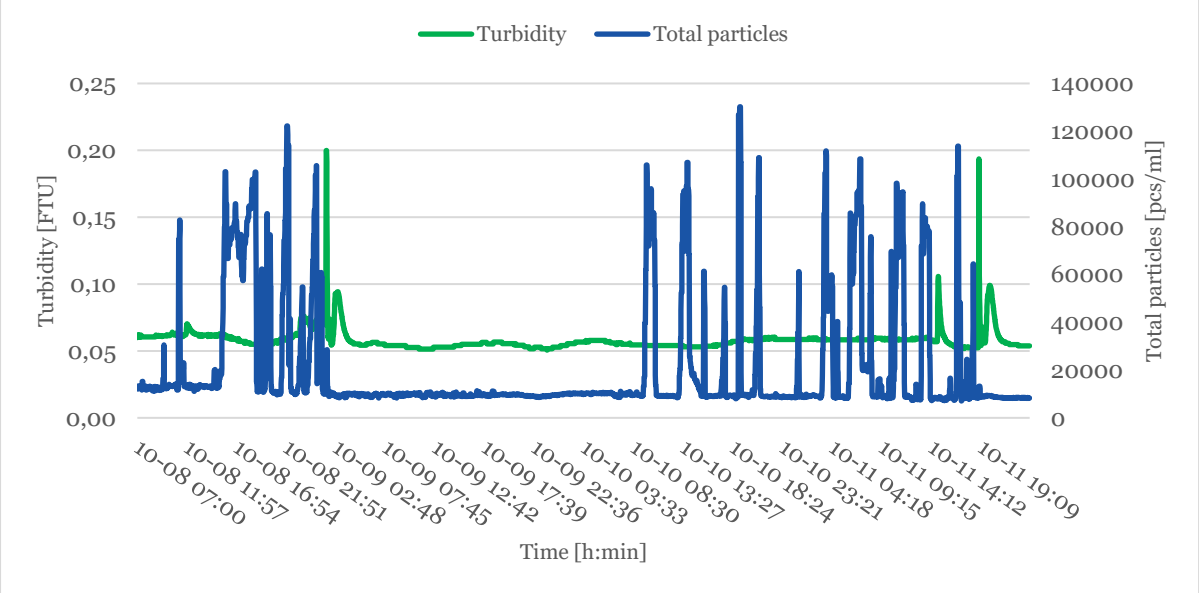

Figure 29. Turbidity and total particles during C.9.

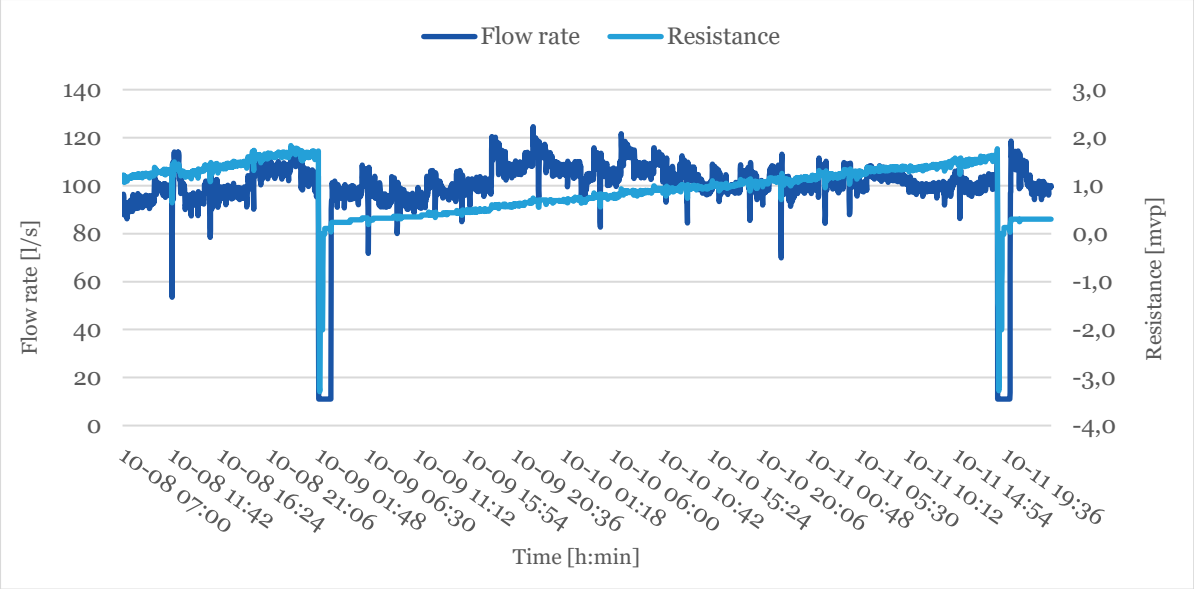

Figure 30. Flow rate and resistance C.9.

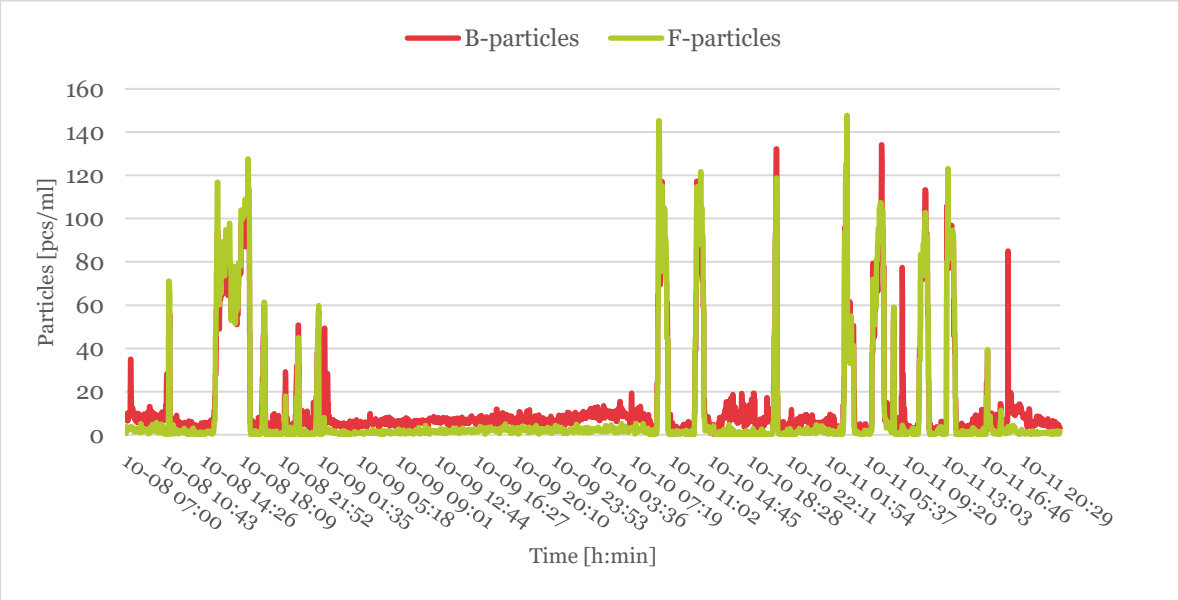

Figure 31. B particles and F-particles during event C.9.

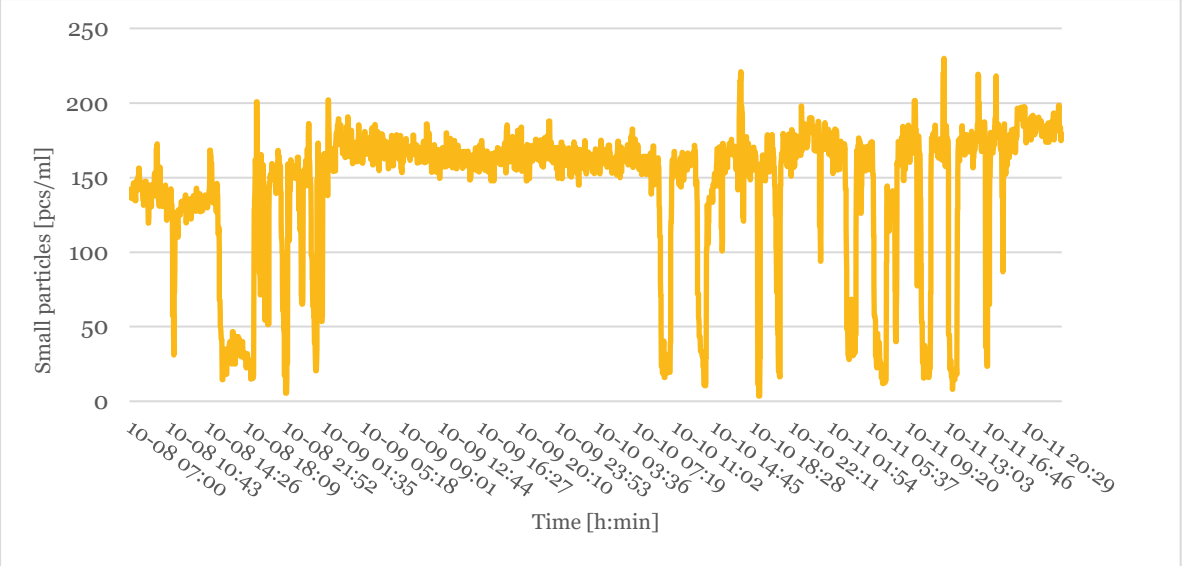

Figure 32. Small particles during event C.9.

The peaks in turbidity are backwashing processes which can be confirmed by the decreased flow rate and resistance. Other than the backwashing processes, the turbidimeter does not register any activity due to values <0,1 FTU.

Total particles and B-and F-particles correlate while small particles follow a different trend. As seen in Figure 33, small particles do not follow the trend, it rather reacts in the opposite way, where the total particles increase, the small particles decrease. Since B- and F-particles are larger particles, they could possibly contribute to small particles not being registered by the particle meter, even though they might be present.

Longer periods where the particle meter showed high activity were also studied. One of these periods, event C.14, is presented below and covers April 16th– April 26th. The turbidity and total particles during event C.14 are shown in Figure 33. The flow rate and filter resistance are shown in Figure 34. B-particles and F-particles during event C.14 are shown in Figure 35 and small particles are shown in Figure 36.

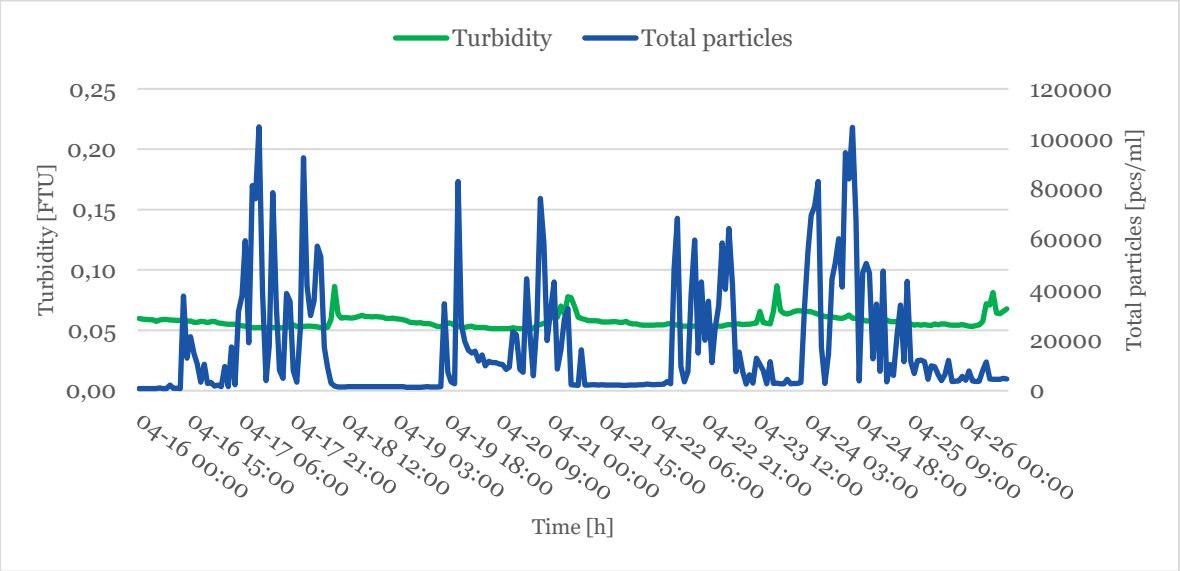

Figure 33. Turbidity and total particles during event C.14.

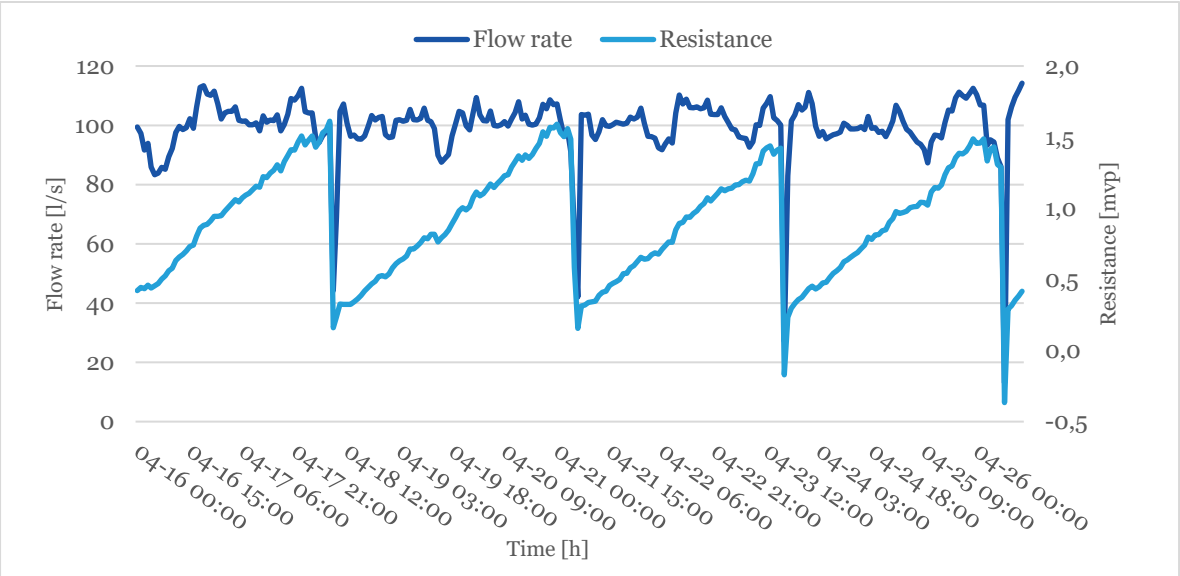

Figure 34. Flow rate and resistance during event C.14.

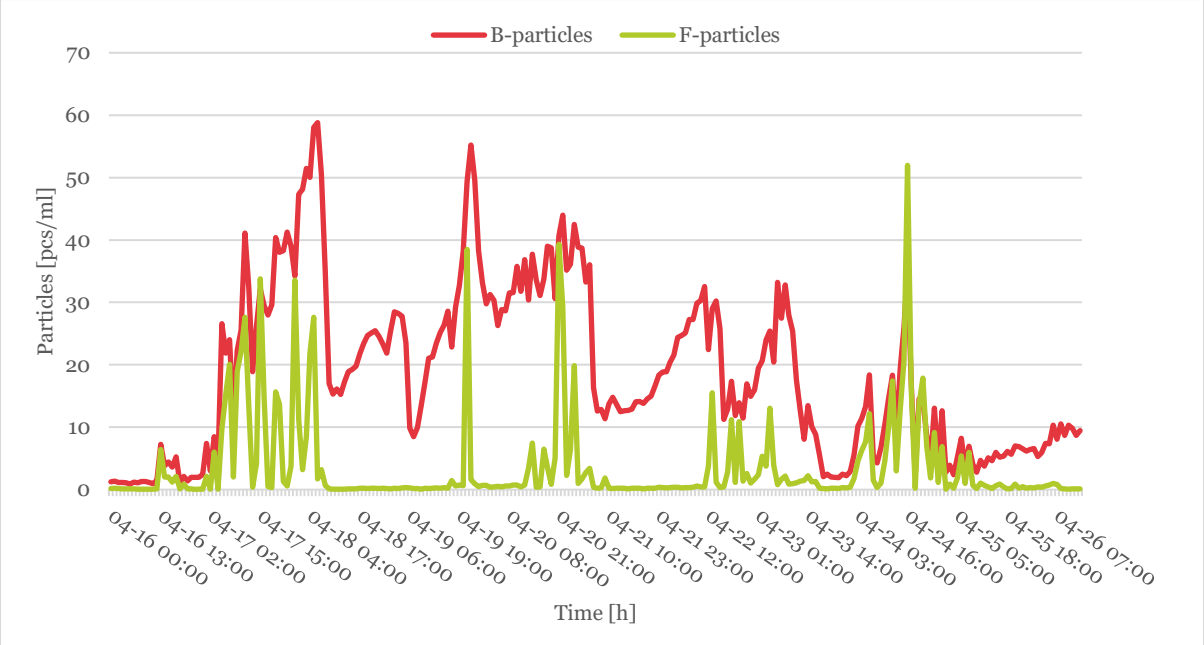

Figure 35. B-particles and F-particles during event C.14.

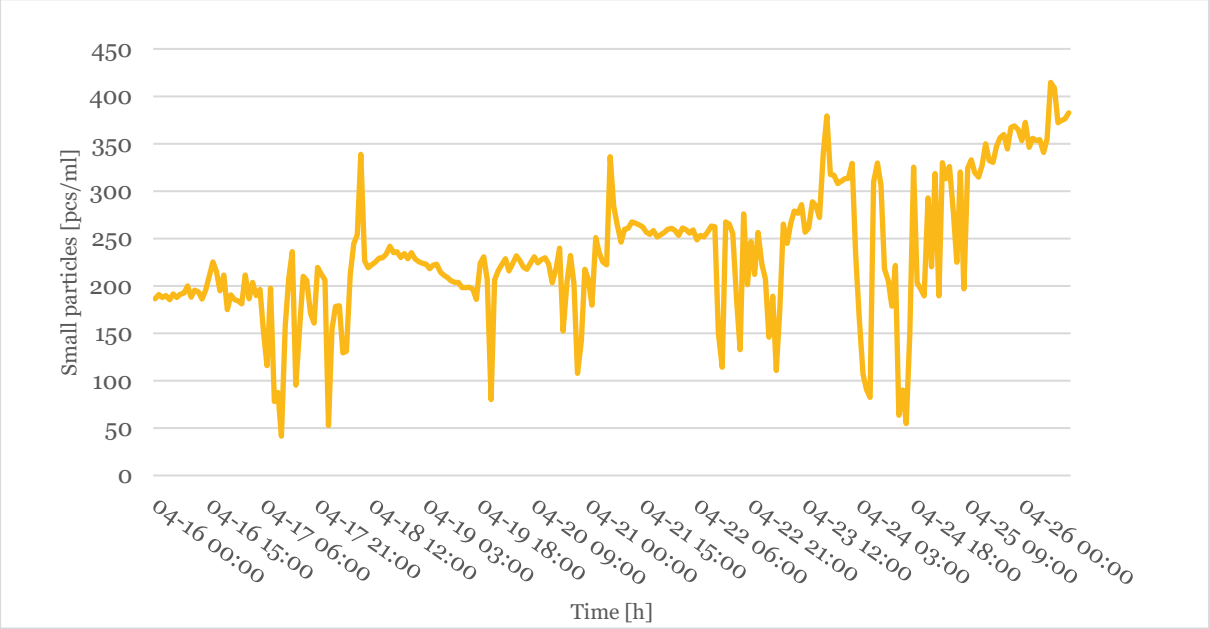

Figure 36. Small particles during event C.14.

The particle meter shows high activity with total particles reaching > 100 000 [pcs/ml], while the turbidimeter shows no activity except during the backwashing processes. The flow rate and resistance trends confirm that the turbidity peaks correspond to the backwashing events. There is a similar pattern between every backwash, a period with little to no activity before a rapid increase and volatile trend of total particles.

F-particles follow the trend of total particles the best. However, the type of particle that dominates during the period is small particles and can be seen in Figure 37. C-particles occur in very small quantities and can therefore be disregarded.

When F-particles and total particles increase, the small particles seem to decrease. Small particles show an overall upgoing trend during the whole period.

Since F-particles best follow the trend of total particles, but in lower concentrations than small particles, it could mean that most particles are uncategorized F-particles. F-particles are fiber-shaped particles and do not usually appear in drinking water, which could mean that there is an ongoing event that brings more F-particles than usual to the raw water intake. The event could be the spring circulation that starts when the water body heats up during spring.

4.2.3 Main findings

Events C.10, C.11, C.12 and C.13 are presented in Appendix II. The dominating particle type during all mentioned events were small particles. However, the particle type that best correlated with total particles were either B-or F-particles or both.

In summary, there are multiple periods where the particle meter shows high activity, and the turbidimeter does not detect anything. The total particles were during all events near and over 100 000 [pcs/ml], which is higher than usual.

The dominating particle category during all events in filter A and C were small particles. Small particles also followed the trend of total particles best in filter A. The reason for the high C-particle values during the events could be false detections since the detection efficiency decreases for particles $< 2\ \mu m$.

On the other hand, the particle category that best correlated with the trend of total particles in filter C were B- and F-particles. A prolonged period with heightened B-particle values could be an indication of a drinking water quality disruption and is therefore an important parameter to keep track of.

Event A.4 occurred in fall and A.5 in spring whereas the events in filter C were mostly from fall and one from spring. It is known that the material in filter A, Filtralite, has a better separation than that of filter C, quartz sand. In filter C, F-and B-particles followed the trend of total particles, which could mean that more larger particles are passing through the filter. The reason small particles followed the trend of total particles best in filter A, could be the material which is finer than that of filter C. No periods where total particles exceeded 100 000 [pcs/ml] were found in filter B, which could be because of the even finer material than filter A.

Surprisingly, F-particles appear to follow the trend of total particles, often together with B-particles, in event C.9, C.10, C.13 and C.14. According to Uponor, some algae appear to register under the F-particle category, which could explain why B-particles and F-particles often follow the same trend. Another reason for the high abundance of F-particles could be spring and fall circulation in Lake Mälaren which mixes particles around the waterbody.

B-particles follow the trend of total particles during event C.9, C.10, C.11, C.12 and C.13. B-particles include algae for instance and algal bloom occur mainly during spring but also in fall. B-particles occur just as F-particles in spring, fall and in December.

4.3 Seasonal variations

The seasonal trends of algae, water temperature, turbidity, total particles, and B-particles are compared in this section.

How algae vary with water temperature is shown in Figure 37. Algae in raw water is measured every week at the laboratory and the water temperature is measured on-line in the raw water intake. Algae correlate with water temperature, except during the summer months. An increase in water temperature and algae can be seen during the spring months when the algal bloom usually takes place. Both temperature and algae show an increasing trend March to May. During May, the algae start to decrease and continue to do so during the summer months. High values of algae occur again in September to November which corresponds to the fall circulation that occur in lakes. The highest values of algae correlate with the highest temperatures in the water intake, which was during October. Interestingly, higher values of algae were recorded in February of 2023, which does not match with the timeline of either algal bloom or fall-and spring circulation.

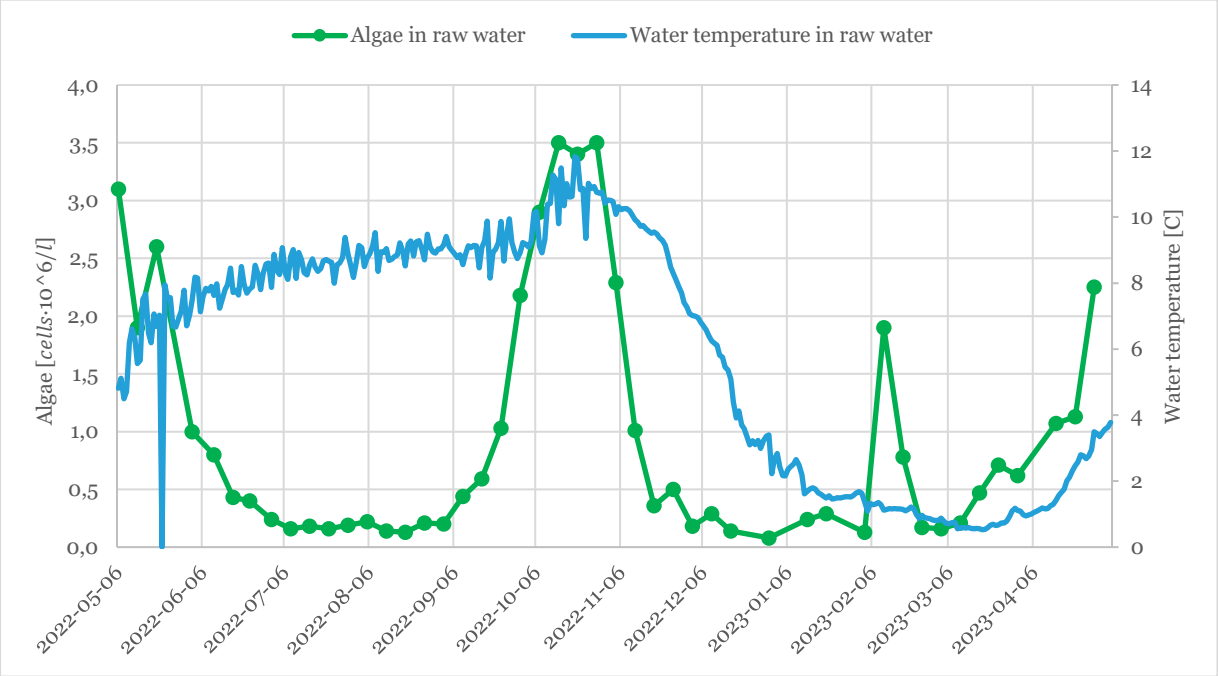

Figure 37. Measured algae from laboratory (one measurement per week) and measured water temperature on-line (average value per day) in the water intake.

In Figure 38, algae concentration is compared to the turbidity in the water intake. Both algae and turbidity are measured at the laboratory. The turbidity trend follows algae concentration relatively closely during January-April, the rest of the year the turbidity seems to be a bit more random compared to algae. The turbidity does not specifically measure algae, moreover, spring- and fall circulation could bring in more particles that increase the turbidity.

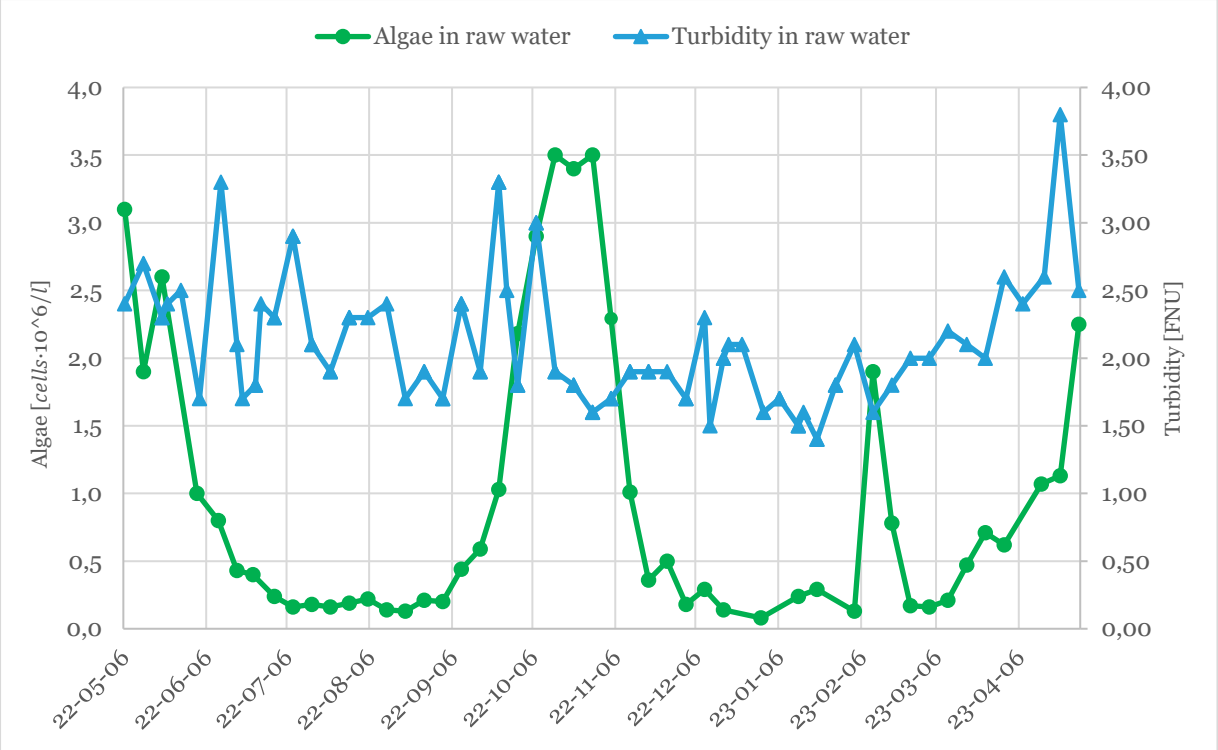

Figure 38. Measured algae and turbidity from the laboratory in the raw water intake.

In Figure 39, a comparison between the algal trend in the raw water to B-particles in the collected sand filtrate was made. B-particles include algae, among other particles, which makes the comparison interesting for the study. Algae in the water intake and B-particles in the sand filtrate are shown to follow approximately the same trend. Since the B-particle category of the particle meter include algae, it supports that the categorization of the instrument is correct.

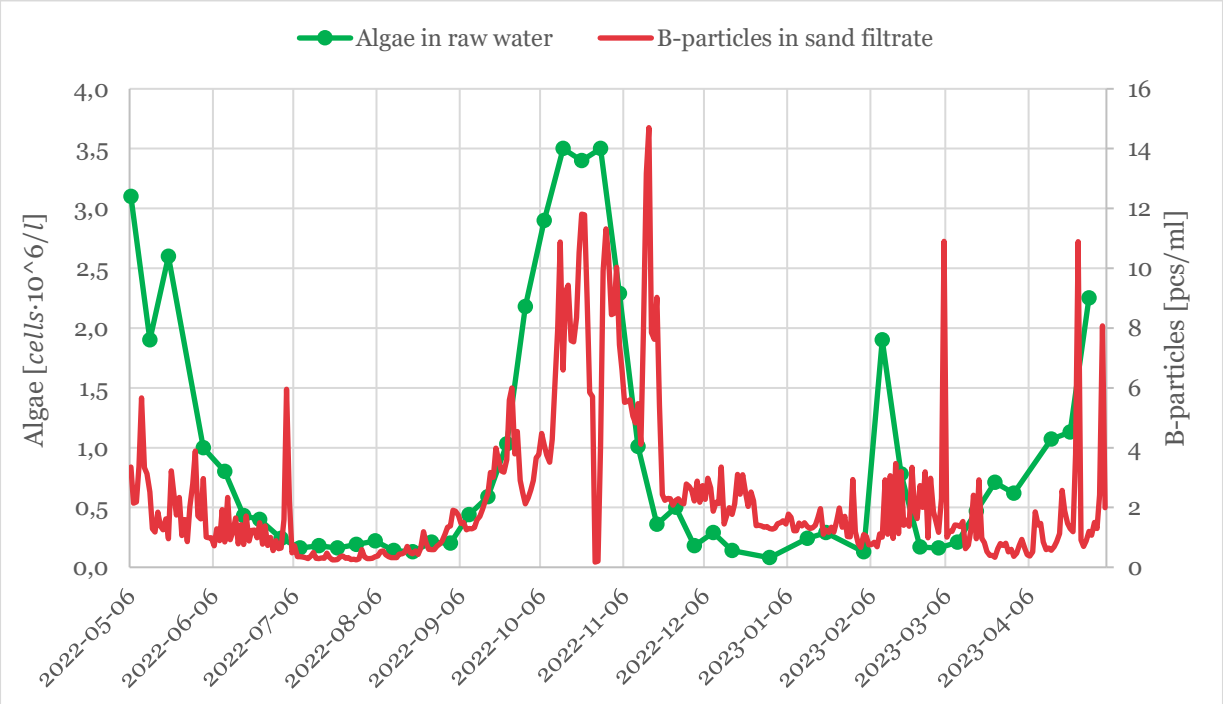

Figure 39. Algae (one measurement per week) in the water intake and B-particles on-line (average value per day) in the collected sand filtrate.

As seen in Figure 40, total particles follow the trend of B-particles during the months March through October. B-particles only account for a very small part of the total particles. Between November and February there are more variations between the two categories. There is a large increase in total particles from early January to early March. The reason for the large increase in particles could be the cold temperature which lessens the effect of coagulation and brings more particles through the rapid filters.

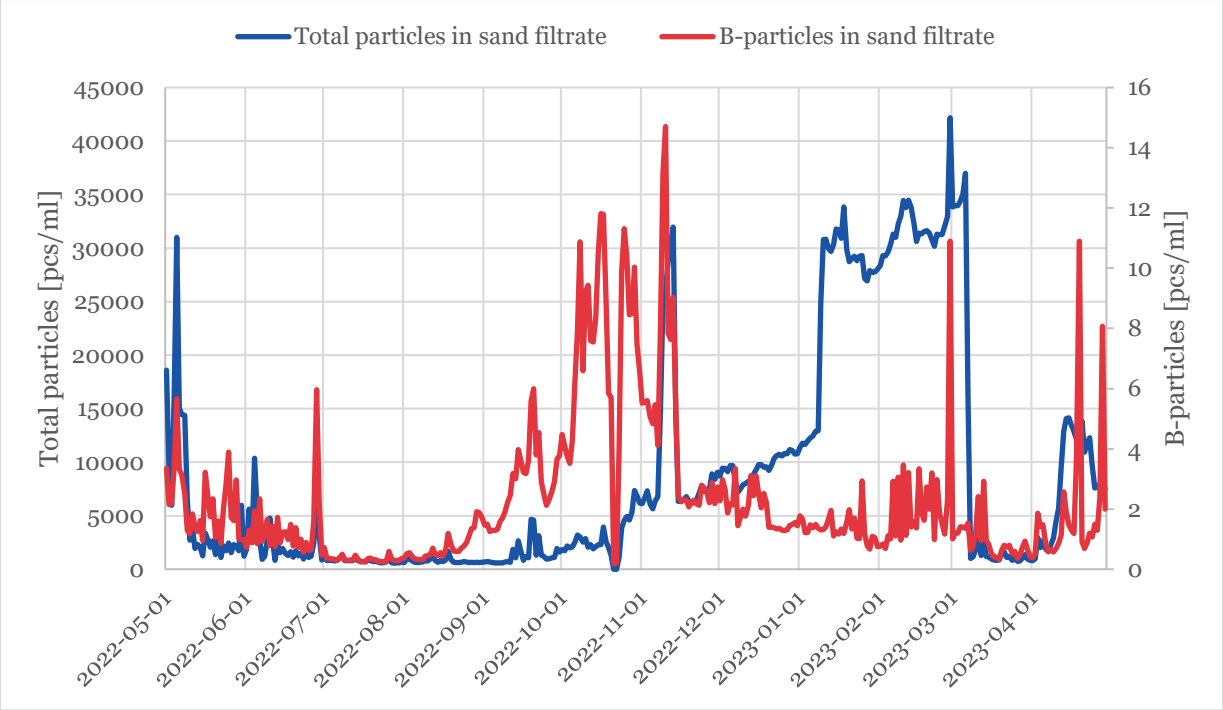

Figure 40. Total particles (average value per day) and B-particles (average value per day) in collected sand filtrate.

4.4 Categorization of the particle meter

The four categories of particles of the particle meter should add up to the total number of particles, however, this has not been the case during the evaluated periods. Only a small part of the total number of particles seems to have been categorized. The reason behind this may be that the AI particle meter has not had enough time to categorize all particles yet. This leads to uncertainty when evaluating the different types of particles. As previously seen in Figure 40, the B-particles seem to have been categorized somewhat correctly since the trend correlates with algae which could mean that the proportions between the different categorized particles are correct even if the numbers are too low.

F-particles and B-particles correlate in some cases, which is explained by different types of algae is categorized under the two categories. Both B-and F-particles could possibly work as an indicator for algal bloom.

One reason for the high values of total particles during all these events could be false detections, that could occur when the particle meter gets fouled. Small particles are as previously mentioned prone to false detections. Another reason for false detections could possibly be fouling, which could disturb the readings.

5 Conclusion

According to this study, the particle meter does not detect a filter breakthrough before the turbidimeter. However, depending on the season, the particle meter follows the turbidimeters trend differently.

During spring, total particles correlate with turbidity, and detects the filter breakthrough at approximately the same time. During the filter breakthroughs between March-June, the total particles, B-particles, and turbidity correlate. The presence of B-particles appears to contribute to the total particles correlating with turbidity.

The examined filter breakthroughs during the fall, September-October, were more difficult to interpret due to the turbidity and total particles not correlating. The reason appeared to be the small particles following the trend of total particles. The particle meter does not detect filter breakthroughs identified by the turbidimeter in fall. During spring and fall, however, multiple periods where total particles > 100 000 [pcs/ml] were found while the turbidity stays below 0,10 FTU. The fact that the particle meter detects such high number of total particles could mean that the rapid filters periodically are unable to separate some type of particulate material which is not registered by the turbidimeter.

The three filters, A, B and C, all consisted of different materials. Eight breakthroughs were found in filter C that had the roughest material. Only three breakthroughs were found in filter A with the finer Filtralite material, and none were found in filter B with the finest Filtralite material. The Filtralite materials have a better separation which is consistent with the number of breakthroughs found. Rapid filter B also has a lower flow rate, which also contributes to the lack of filter breakthroughs found. The filters running time also affects the possibility of a turbidity breakthrough.

B-particles correlate well with algae in raw water. The particle meter could possibly contribute to a fast indication on when the algal bloom starts in Lake Mälaren compared to laboratory tests, which normally are conducted only once a week.

The dominating particle category during all studied events were small particles. However, which particle that best followed the trend of total particles varied. In filter A, the particle category that best followed the trend of total particles were small particles, and in filter C it was B-and F-particles. C-particles did not occur in any significant amounts during the evaluated periods. However, F-particles did occur in larger amounts during some of the events, and often together with B-particles. The reason B-and F-particles sometimes follow the same trend could be that particles, such as algae, could have been categorized into the two categories simultaneously.

The categorization of the different particles of the particle meter does not seem to be completely ready. The number of total particles is in most cases much higher than the total of B-, C-, F- and small particles. This leads to difficulty in interpreting and using the produced data. Another uncertainty is the possibly false readings that could occur when the particle meter gets fouled.

6 References

[1] Livsmedelsverket. Dricksvattenkvalitet 2022. https://www.livsmedelsverket.se/livsmedel-och-innehall/dricksvatten/dricksvattenkvalitet (accessed October 1, 2023).

[2] Norrvatten. Dricksvattenproduktion n.d. https://www.norrvatten.se/dricksvatten/dricksvattenproduktion/ (accessed March 21, 2023).

[3] Norrvatten. Reningsprocessen n.d. https://www.norrvatten.se/dricksvatten/dricksvattenproduktion/reningsprocessen/ (accessed March 21, 2023).

[4] Berghult B, Bergstedt O, Blom A, Danielsson H, Elfström Broo A, Engdahl M, et al. Dricksvattenteknik 3, Ytvatten (U8). Stockholm: Svenskt Vatten AB; 2010.

[5] Popek E. Sampling and Analysis of Environmental Chemical Pollutants. 2nd ed. Amsterdam: Elsevier; 2018.

[6] Persson PO, Nilson L, Östman A. Miljöskyddsteknik - Strategier & teknik för miljöskydd. Stockholm: Inst. för ingenjörspedagogik Kungliga Tekniska Högskolan; 2018.

[7] Norrvatten. PFAS-rening med hjälp av flotation 2023. http://www.norrvatten.se/om-norrvatten/nyheter/nyhetsarkiv/nyheter-2023/pfas-rening-med-hjalp-av-flotation/ (accessed September 30, 2023).

[8] Jekel M, Gimbel R. Water, 4. Treatment by Flocculation and Filtration 2016. https://doi.org/10.1002/14356007.028_015.pub2.

[9] Johansson T, Sekizovic I. Filtralite 2021 Unpublished.

[10] Filtralite. Filtralite® Pure | Drupal n.d. https://www.filtralite.com/sv/losningar/filtraliter-pure (accessed April 22, 2023).

[11] Omar AFB, MatJafri MZB. Turbidimeter Design and Analysis: A Review on Optical Fiber Sensors for the Measurement of Water Turbidity 2009;9:8311–35. https://doi.org/10.3390/s91008311.

[12] Lawler DM. Turbidity, Turbidimetry, and Nephelometry☆. In: Worsfold P, Poole C, Townshend A, Miró M, editors. Encycl. Anal. Sci. Third Ed., Oxford: Academic Press; 2016, p. 152–63. https://doi.org/10.1016/B978-0-12-409547-2.11006-6.

[13] HF scientific. Owner's manual MicroTOL Series Turbidimeter 2014.

[14] Hach. 1720E Low Range Turbidimeter USER MANUAL 2016.

[15] Grafe F. Ackrediteringens omfattning. SWEDAC, 2023.

[16] Uponor. User Handbook for Uponor Water Quality Measurement System UWQMS. Unpublished document, 2021.

[17] Uponor. Säker dricksvattenkvalitet n.d. https://www.uponor.com/sv-se/infra/service/water-monitoring-services/water-quality-monitoring-service (accessed April 28, 2023).

[18] Koppanen M, Kesti T, Kokko M, Rintala J, Palmroth M. An online flow-imaging particle counter and conventional water quality sensors detect drinking water contamination in the presence of normal water quality fluctuations. Water Res 2022;213:118149. https://doi.org/10.1016/j.watres.2022.118149.

[19] Holden J. Introduction to Physical Geography and the Environment. 4th ed. Harlow, United Kingdom: Pearson; 2017.

[20] Sveriges meteorologiska och hydrologiska institut. Vattentemperatur i sjöar 2021. https://www.smhi.se/kunskapsbanken/hydrologi/sveriges-sjoar/vattentemperatur-i-sjoar-1.172778 (accessed May 12, 2023).

[21] Aneer G, Löfgren S. ALGBLOMNING - Några frågor och svar. Länsstyrelsen i Stockholms län; 2007.

Appendix I Rapid Filter C - Filter breakthroughs

Turbidity and total particles during filter breakthrough C.14, between September 19th – 20th, can be seen in Figure 41.

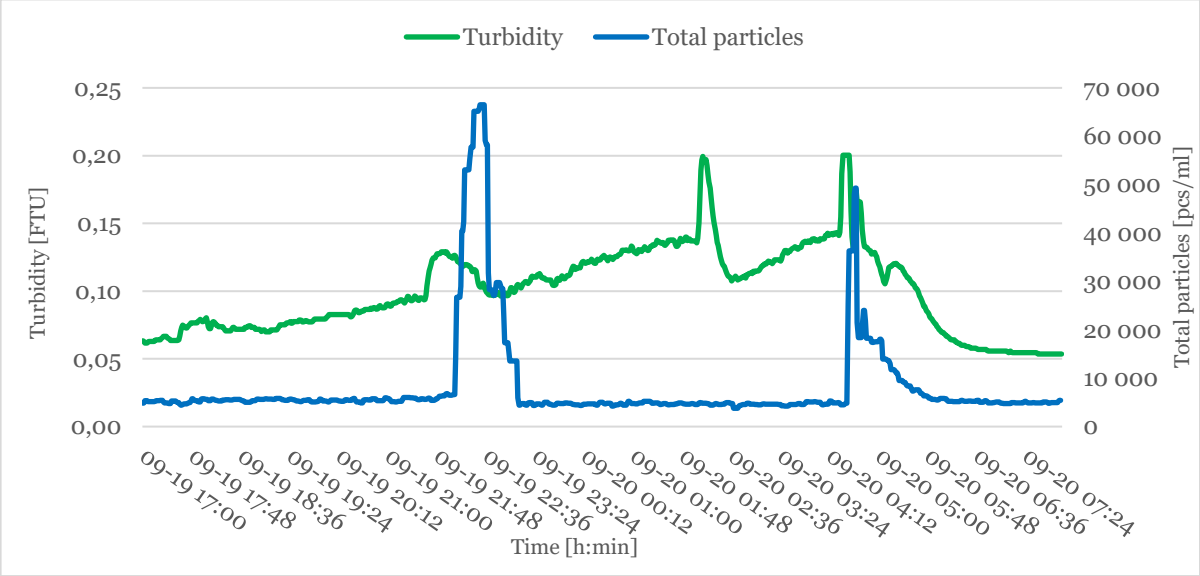

Figure 41. Turbidity and total particles during event C.4.

Flow rate and resistance around filter breakthrough C.4 is shown in Figure 42.

Figure 42. Flow rate and resistance during event C.4.

B-particles and small particles around the filter breakthrough are shown in Figure 43.

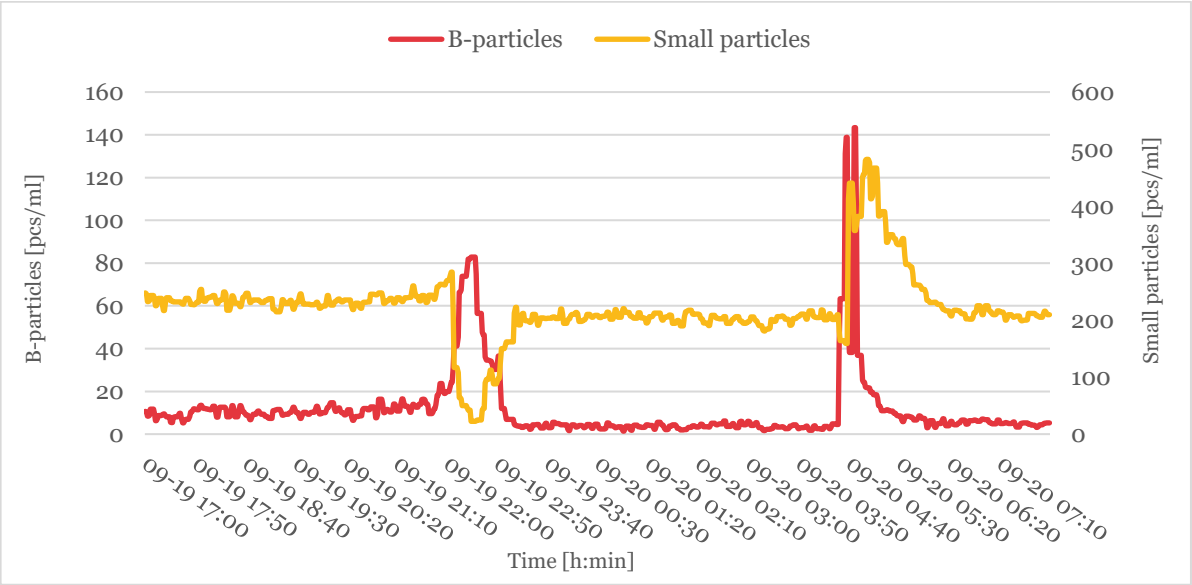

Figure 43. B-particles and small particles during event C.4.

Turbidity and total particles during filter breakthrough C.6, on March 10th, can be seen in Figure 44.

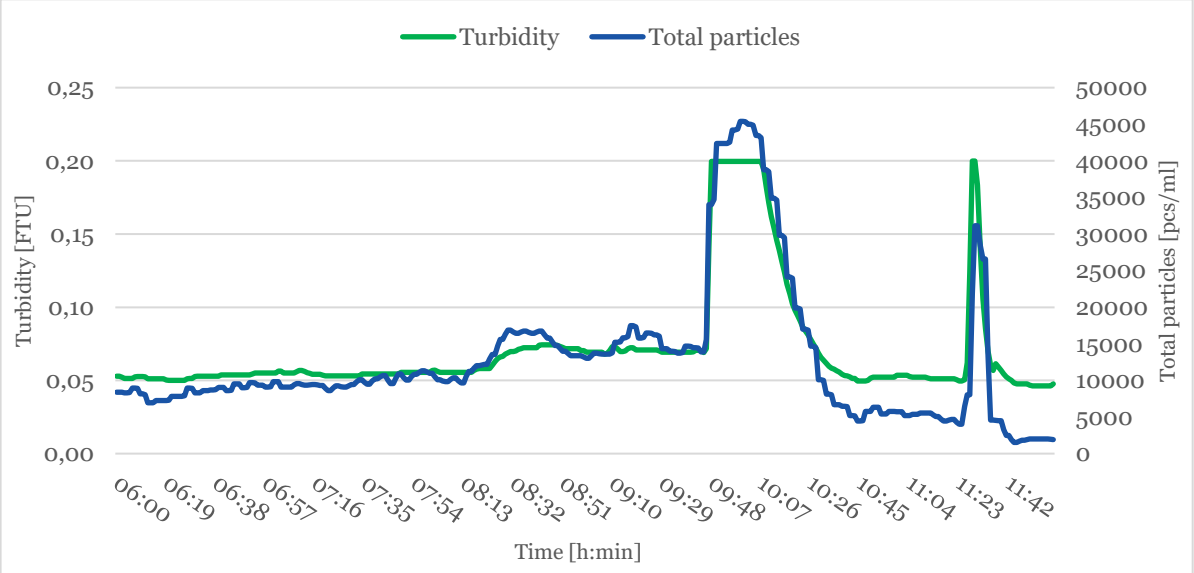

Figure 44. Turbidity and total particles during event C.6 10th of March 2023.

Flow rate and resistance around filter breakthrough C.6 is shown in Figure 45.

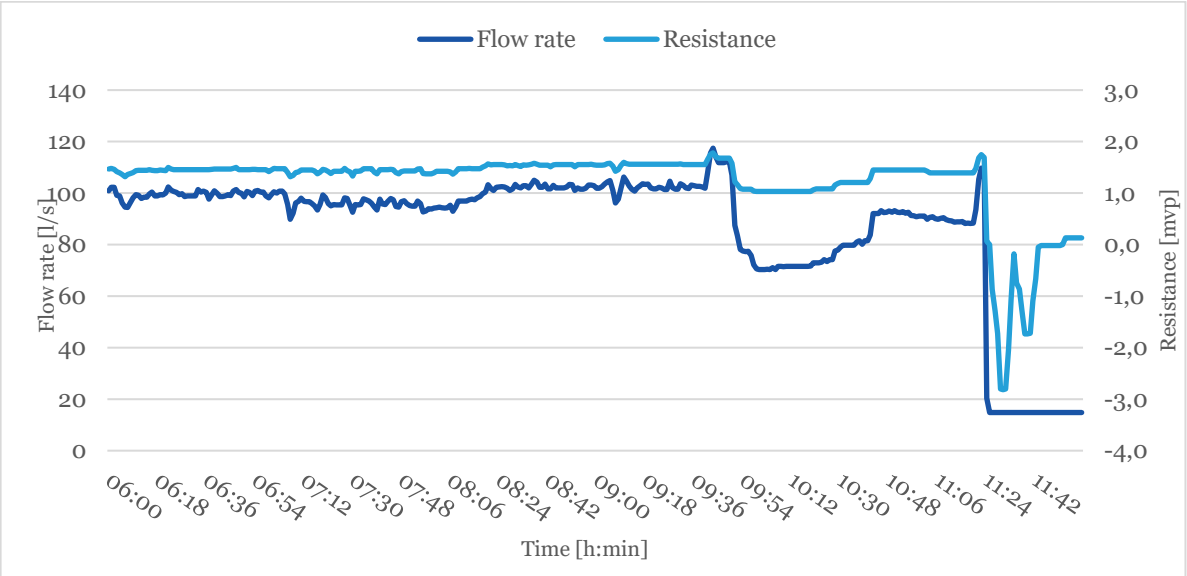

Figure 45. Flow rate and resistance during event C.6.

B-particles and small particles around the filter breakthrough are shown in Figure 46.

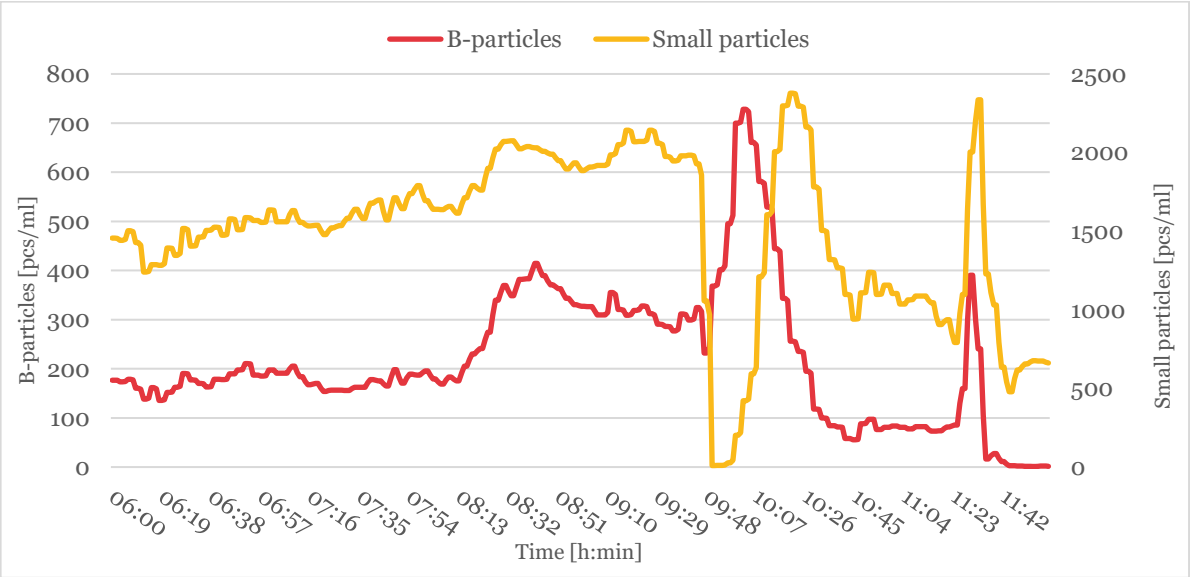

Figure 46. B-particles and small particles during event C.6.

Turbidity and total particles during filter breakthrough C.7 and C.8, between April 4th-5th, can be seen in Figure 47.

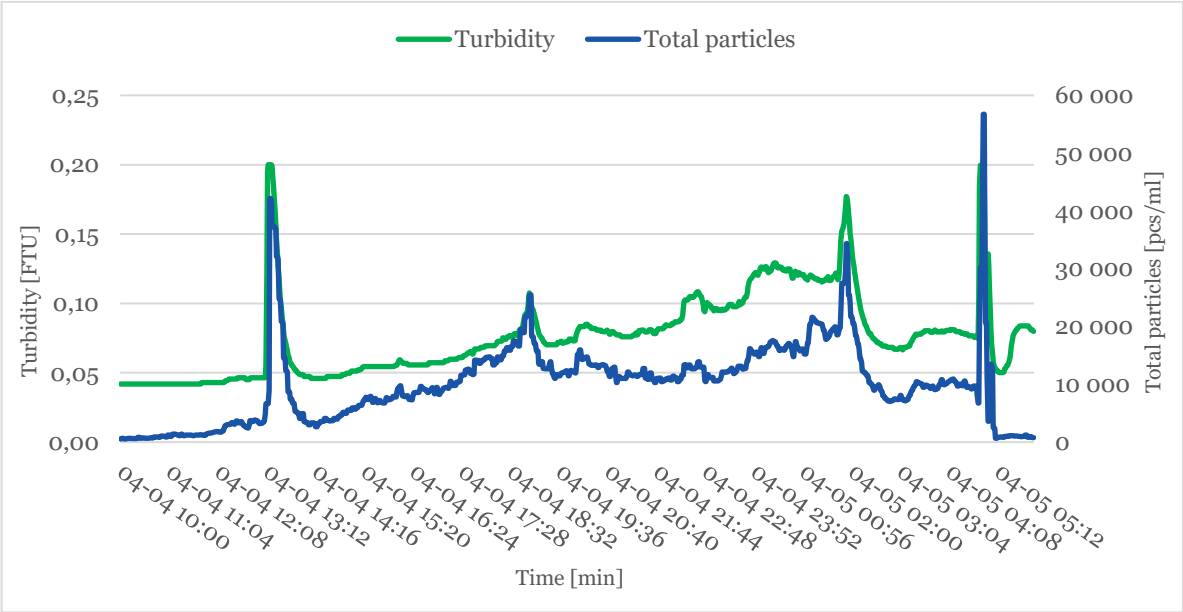

Figure 47. Turbidity and total particles during event C.7 and C.8 during 4-5 April 2023.

Flow rate and resistance around filter breakthrough C.6 is shown in Figure 48.

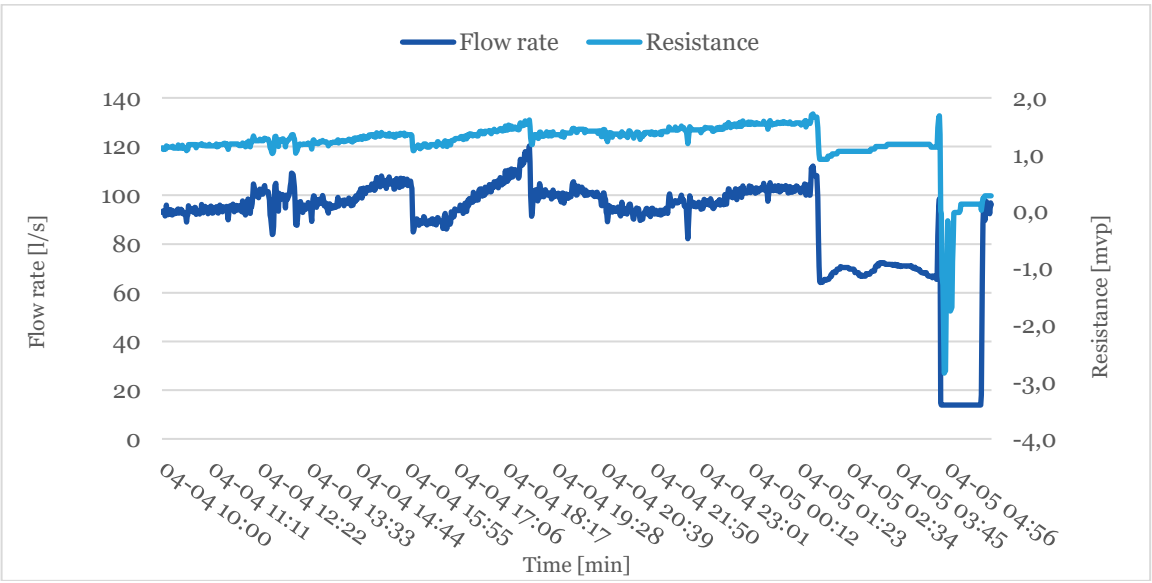

Figure 48. Flow rate and resistance during event C.7 and C.8.

B-particles and small particles around filter breakthrough C.7 and C.8 are shown in Figure 49.

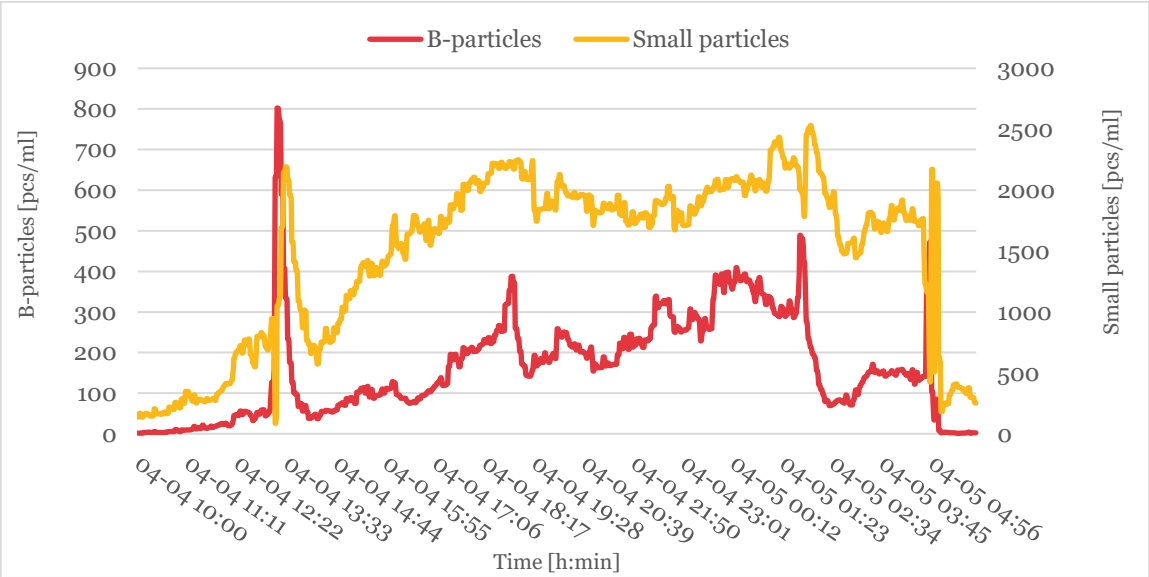

Figure 49. B-particles and small particles during event C.7 and C.8.

Appendix II Rapid Filter C - Drastic increase in number of particles

Turbidity and total particles during event C.10, which covers the period October 31st - November 13th, 2022, can be seen in Figure 50.

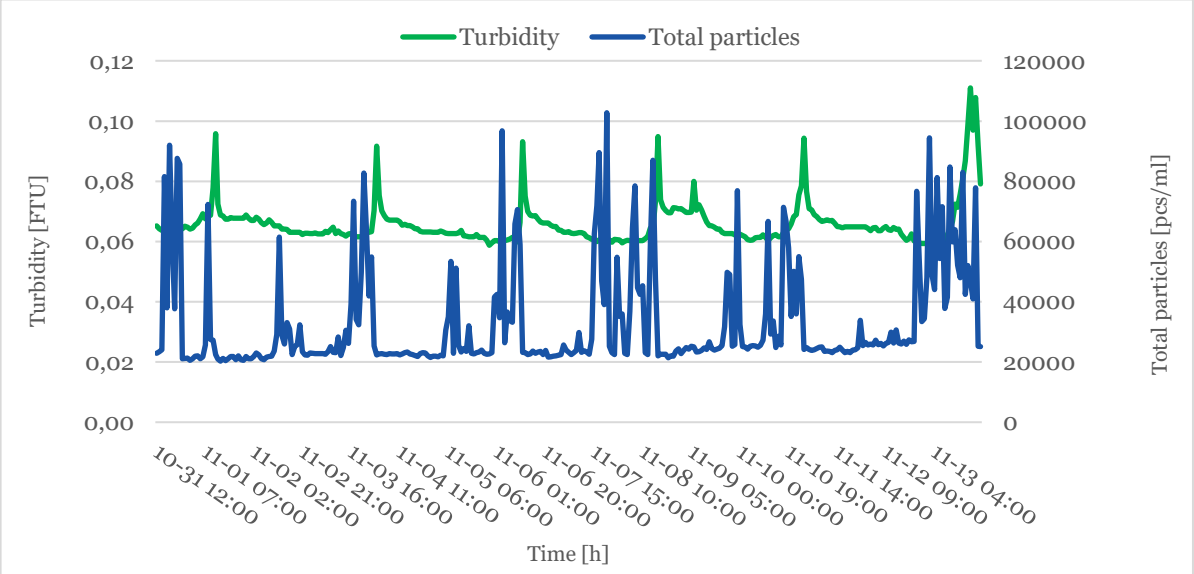

Figure 50. Turbidity and total particles during event C.10.

Flow rate and resistance during the period is shown in Figure 51.

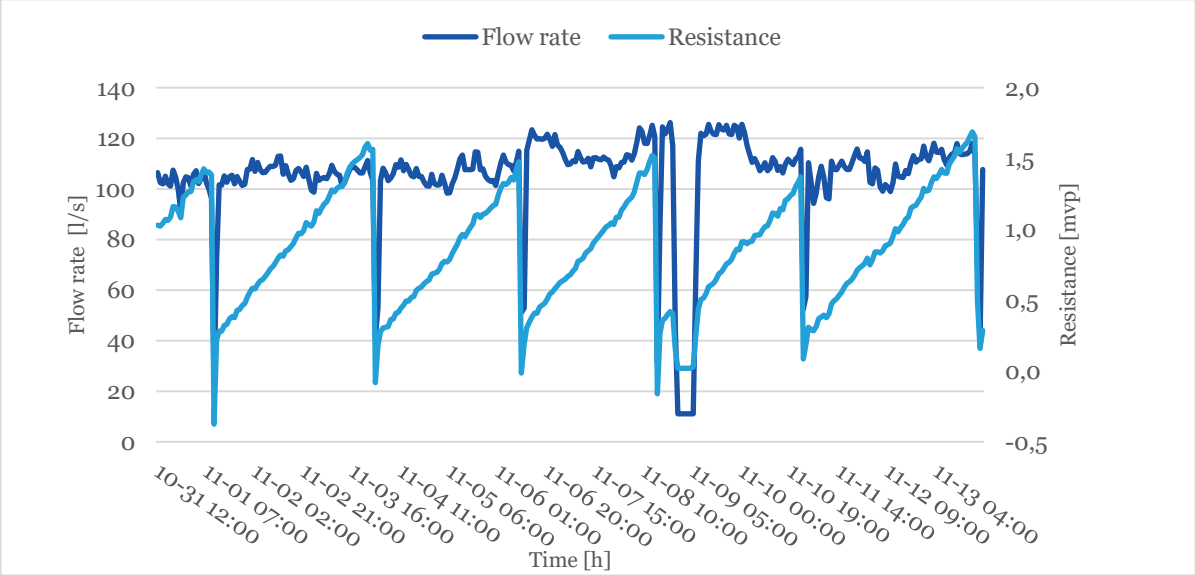

Figure 51. Flow rate and resistance during event C.10.

How small particles vary during event C.10 is shown in Figure 52 and B-and F-particles are shown in Figure 53. C-particles occurred in such small quantities, < 1 $[pcs/ml]$, and are not included.

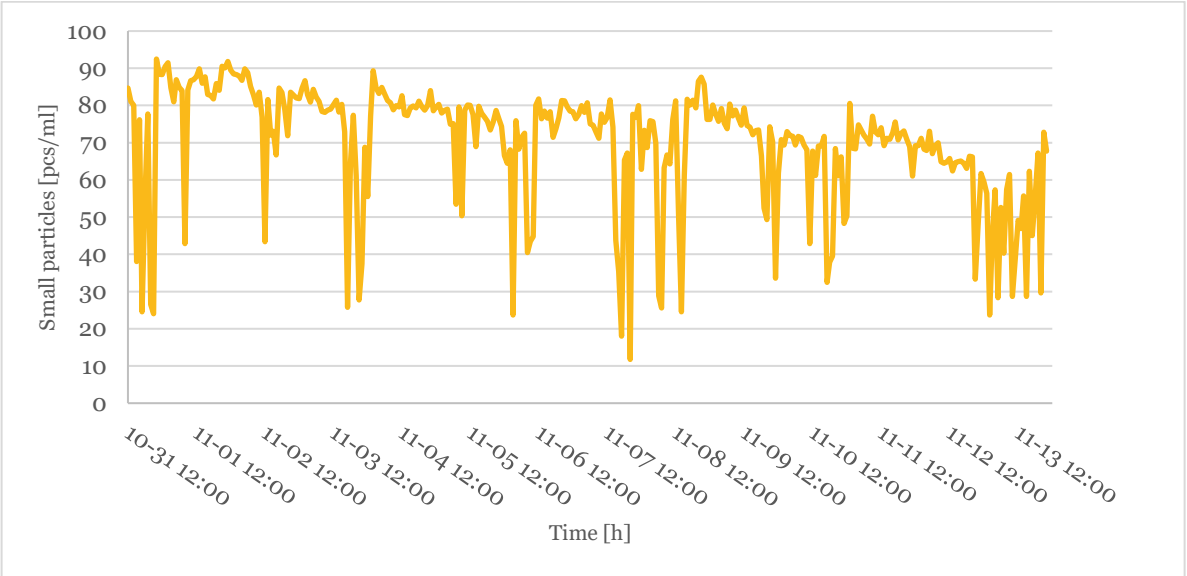

Figure 52. Small particles during event C.10.

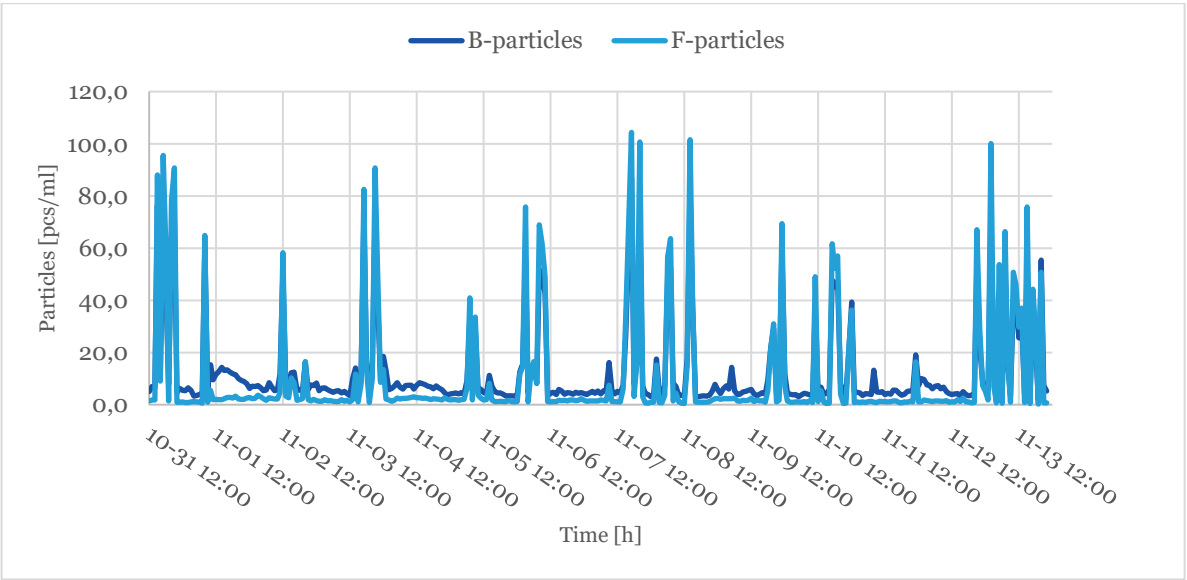

Figure 53. B- and F-particles during event C.10.

Turbidity and total particles during event C.10, which covers the period November 25th -26th, 2022, can be seen in Figure 54.

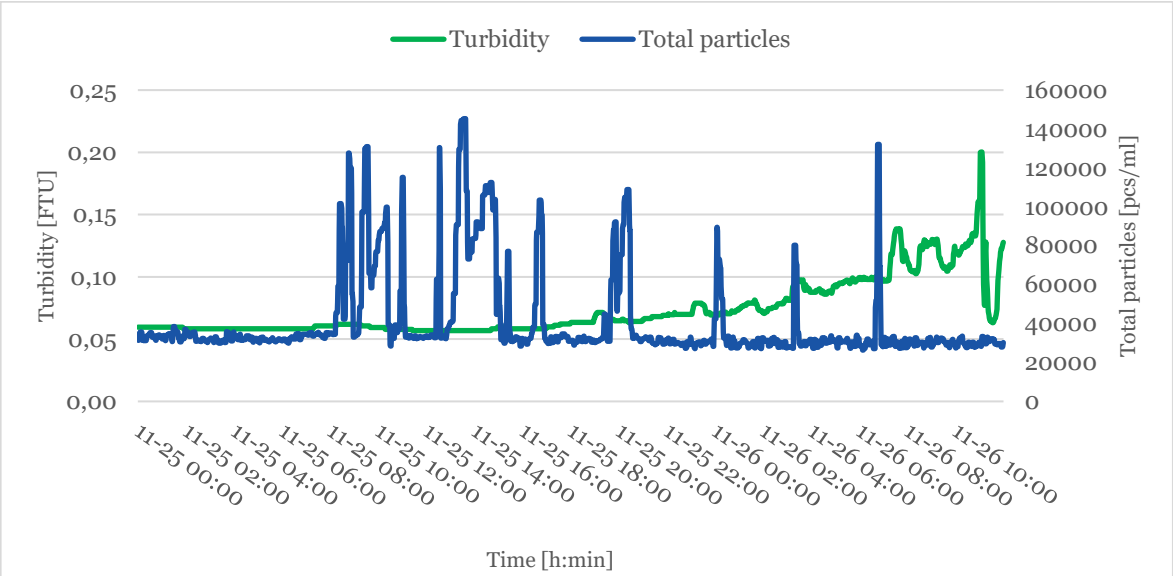

Figure 54. Turbidity and total particles during event C.11.

Flow rate and resistance during the period is shown in Figure 55.

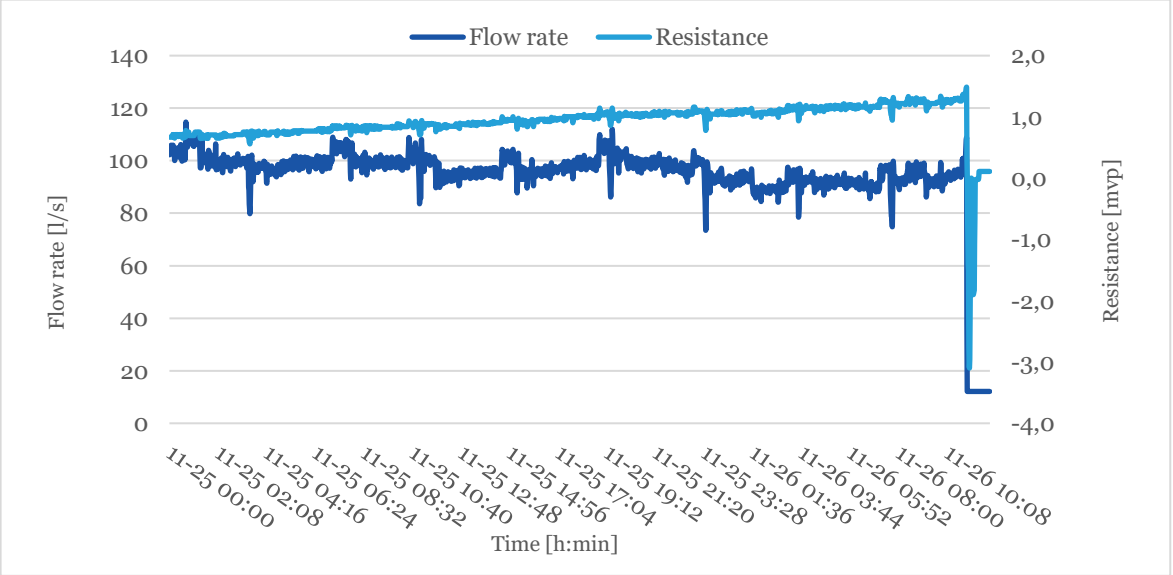

Figure 55. Flow rate and resistance during event C.11.

How small particles vary during event C.10 is shown in Figure 56 and B-and F-particles are shown in Figure 57. C-particles occurred in such small quantities, < 1 $[pcs/ml]$, and are not included.

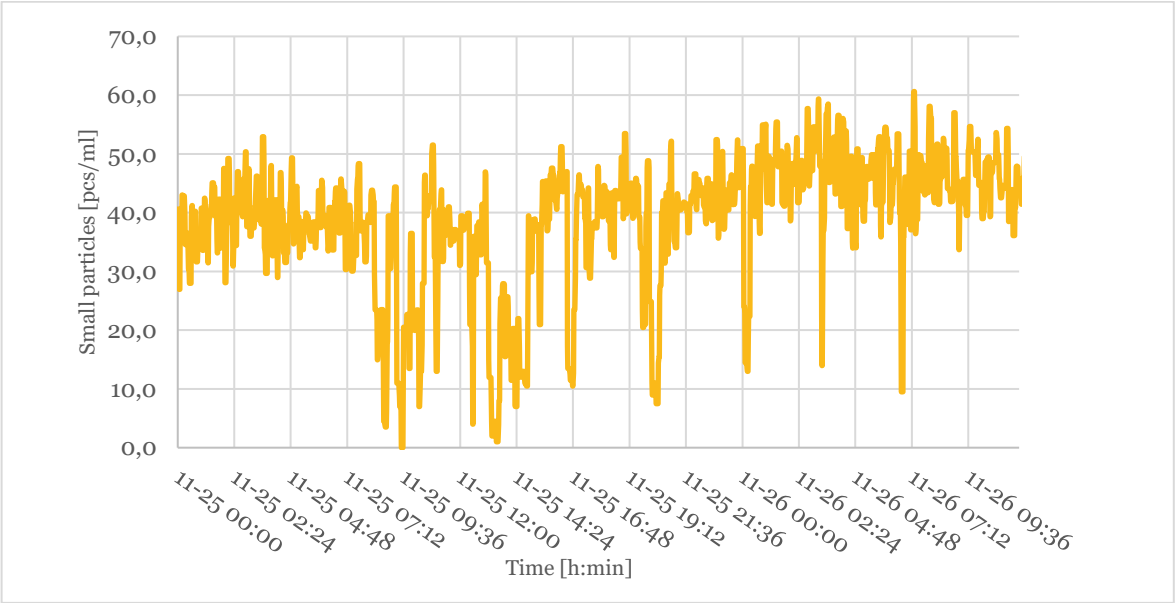

Figure 56. Small particles during event C.11.

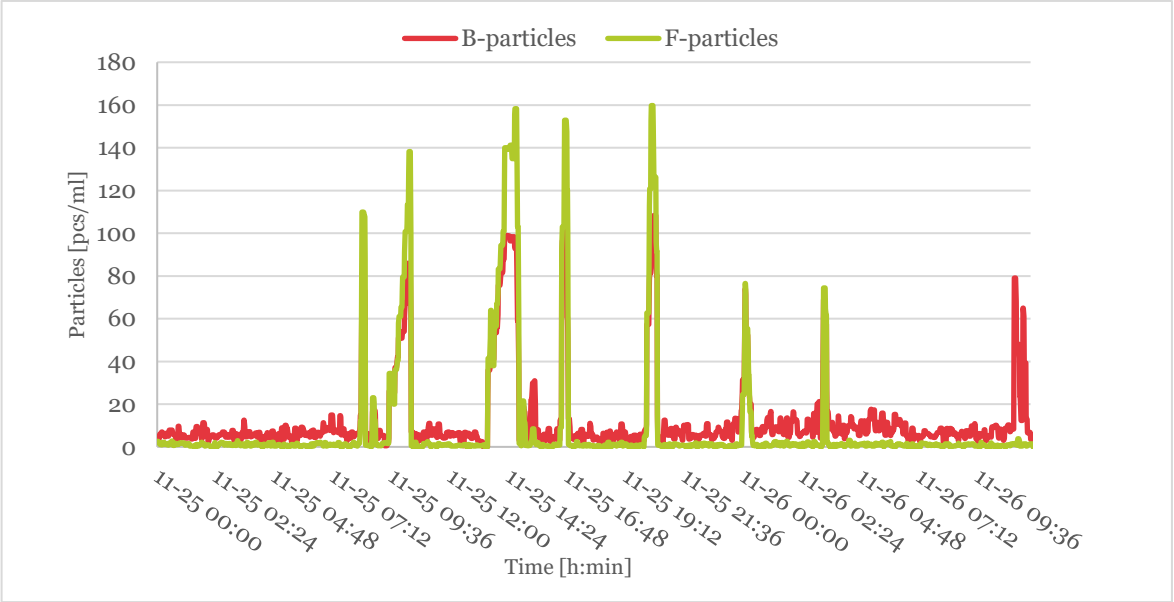

Figure 57. B- and F-particles during event C.11.

Turbidity and total particles during event C.12, which covers the period December 9th -12th, 2022, can be seen in Figure 58.

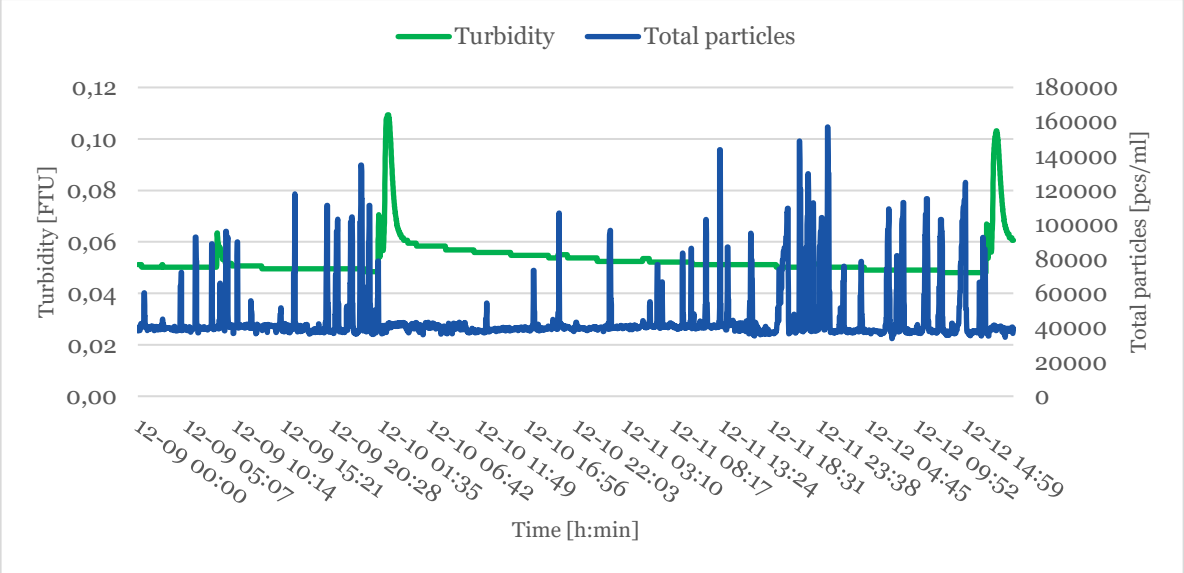

Figure 58. Turbidity and total particles during event C.12.

Flow rate and resistance during the period is shown in Figure 59.

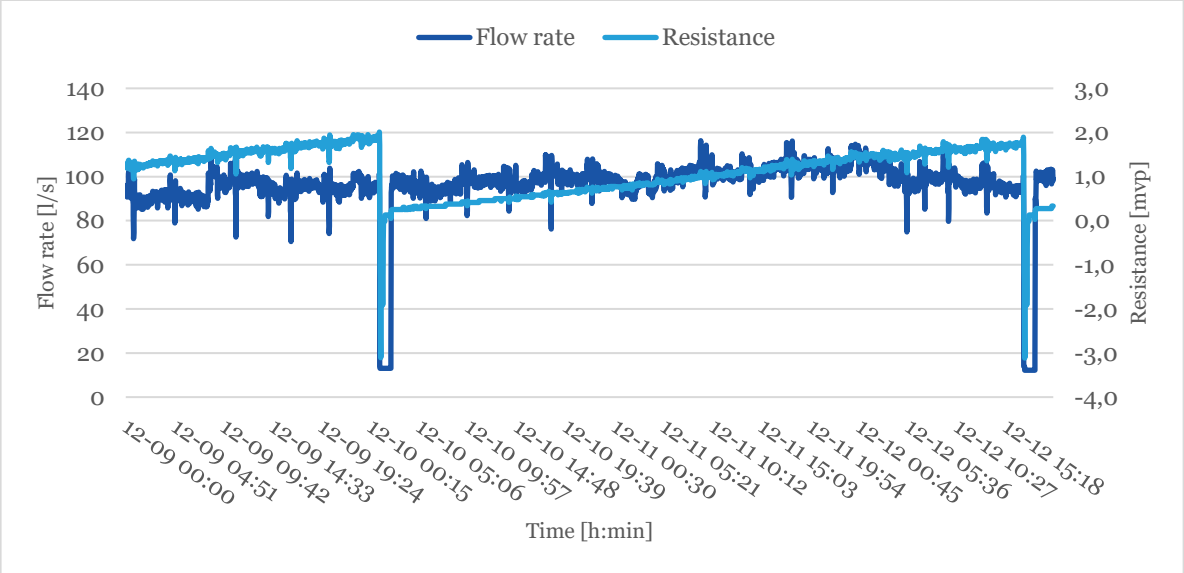

Figure 59. Flow rate and resistance during event C.12.

How small particles vary during event C.12 is shown in Figure 60. B-particles are shown in Figure 61 and F-particles are shown in Figure 62. C-particles occurred in such small quantities, < 1 $[pcs/ml]$, and are not included.

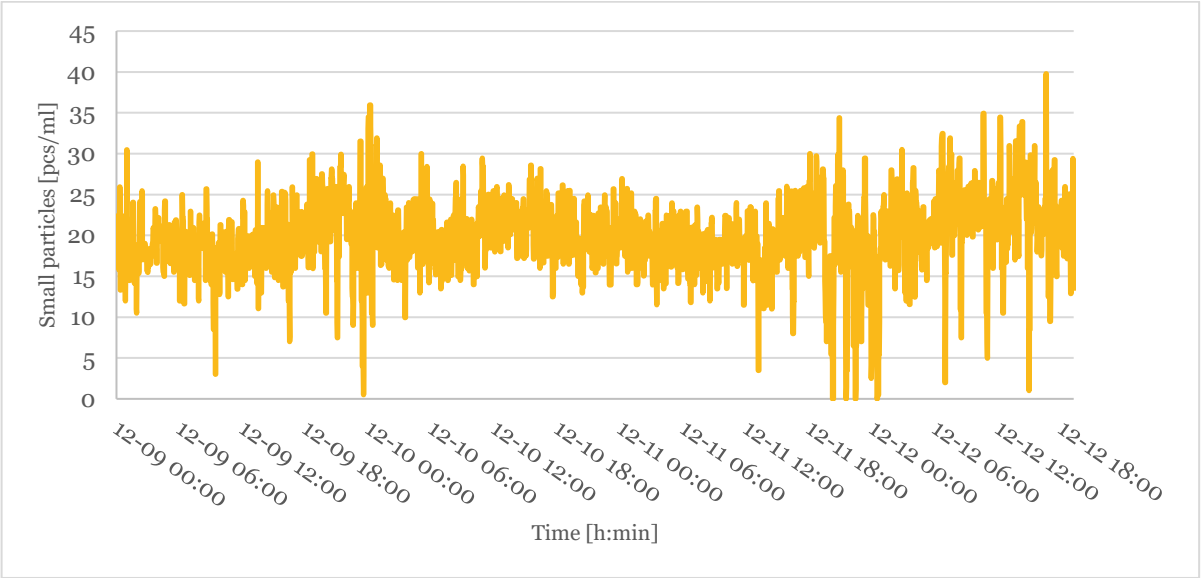

Figure 60. Small particles during event C.12.

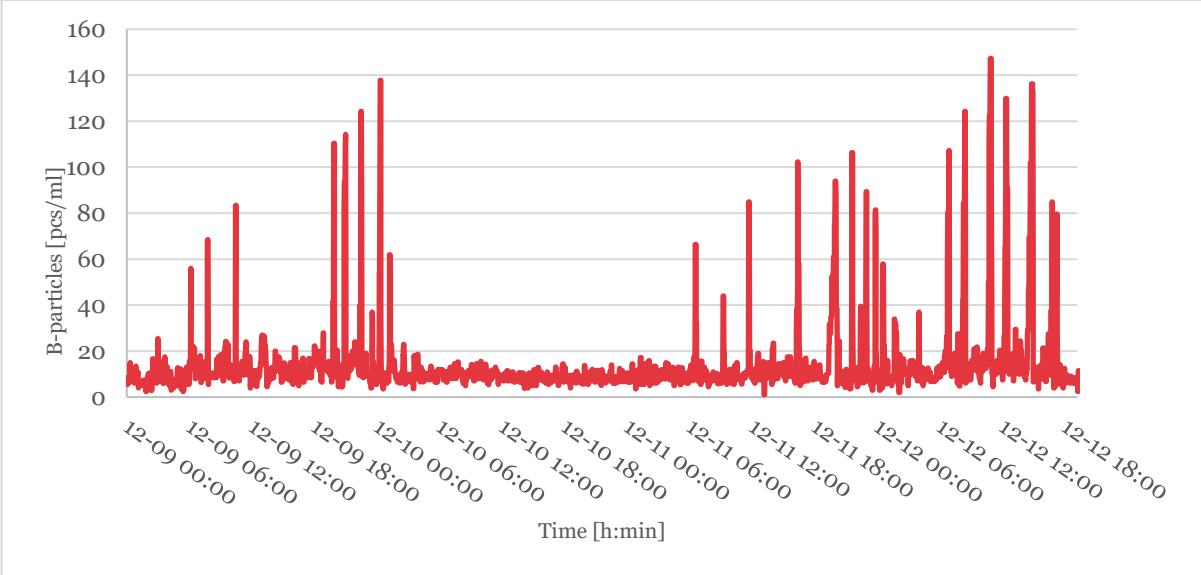

Figure 61. B-particles during event C.12.

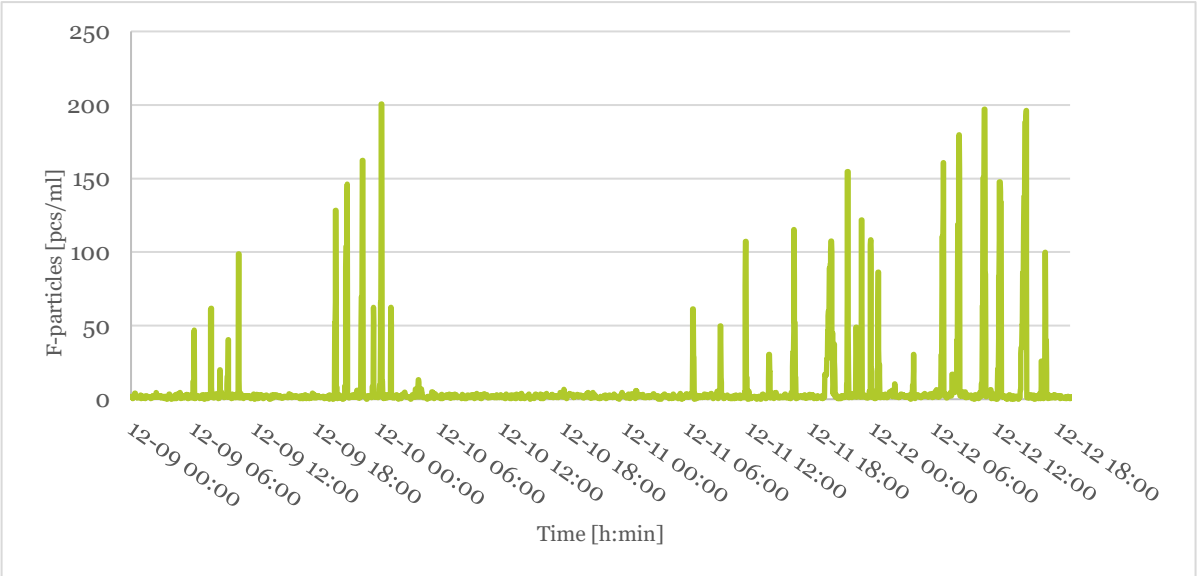

Figure 62. F-particles during event C.12.

Turbidity and total particles during event C.13, which covers the period December 17th -20th, 2022, can be seen in Figure 63.

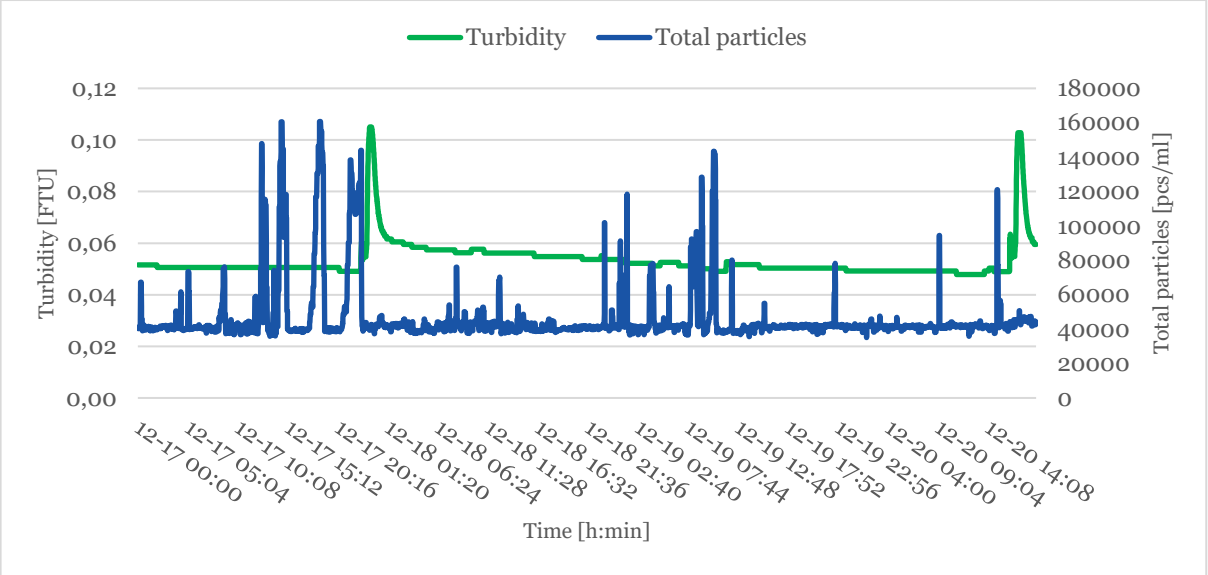

Figure 63. Turbidity and total particles during event C.13.

Flow rate and resistance during the period is shown in Figure 64.

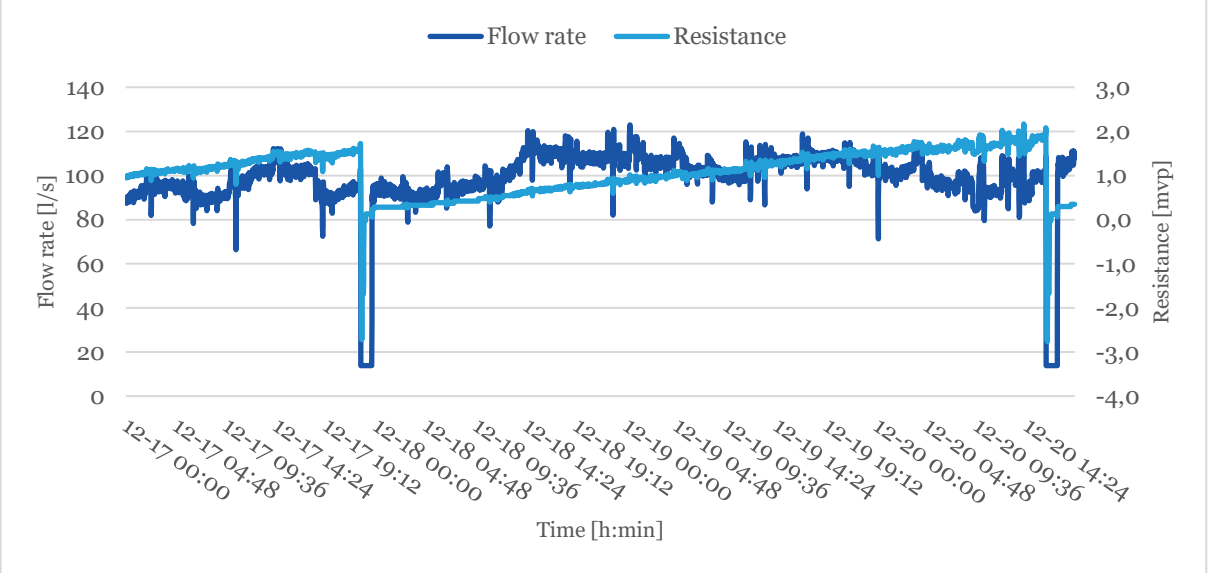

Figure 64. Flow rate and resistance during event C.13.

How small particles vary during event C.13 is shown in Figure 65. B-particles are shown in Figure 66 and F-particles are shown in Figure 67. C-particles occurred in such small quantities, < 1 $[pcs/ml]$, and are not included.

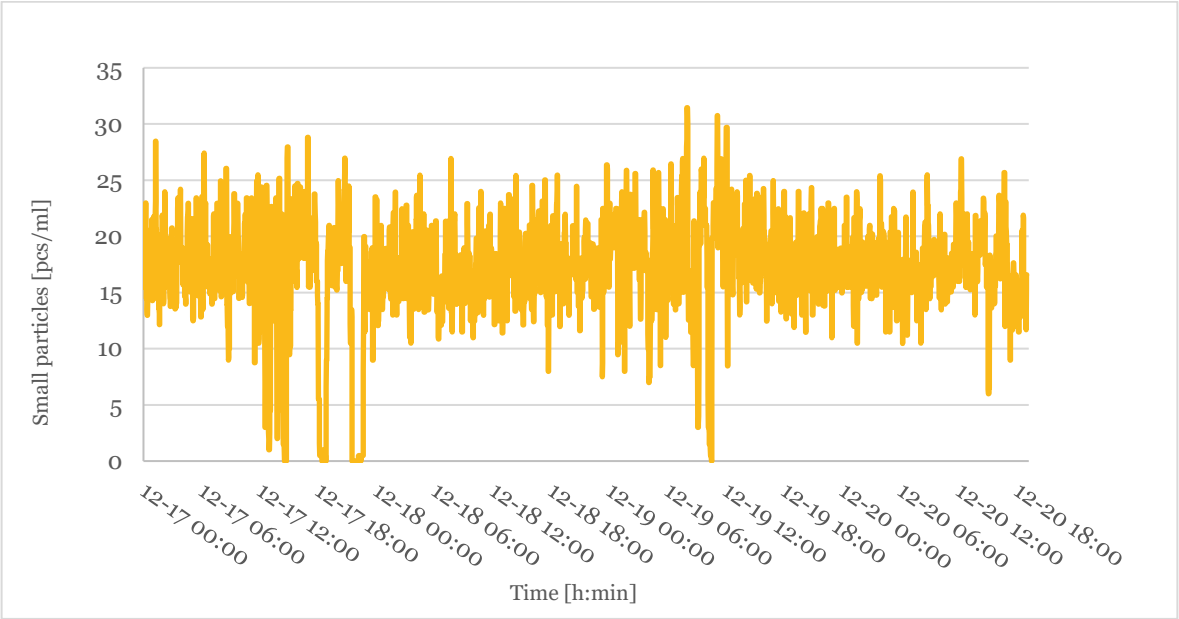

Figure 65. Small particles during event C.13.

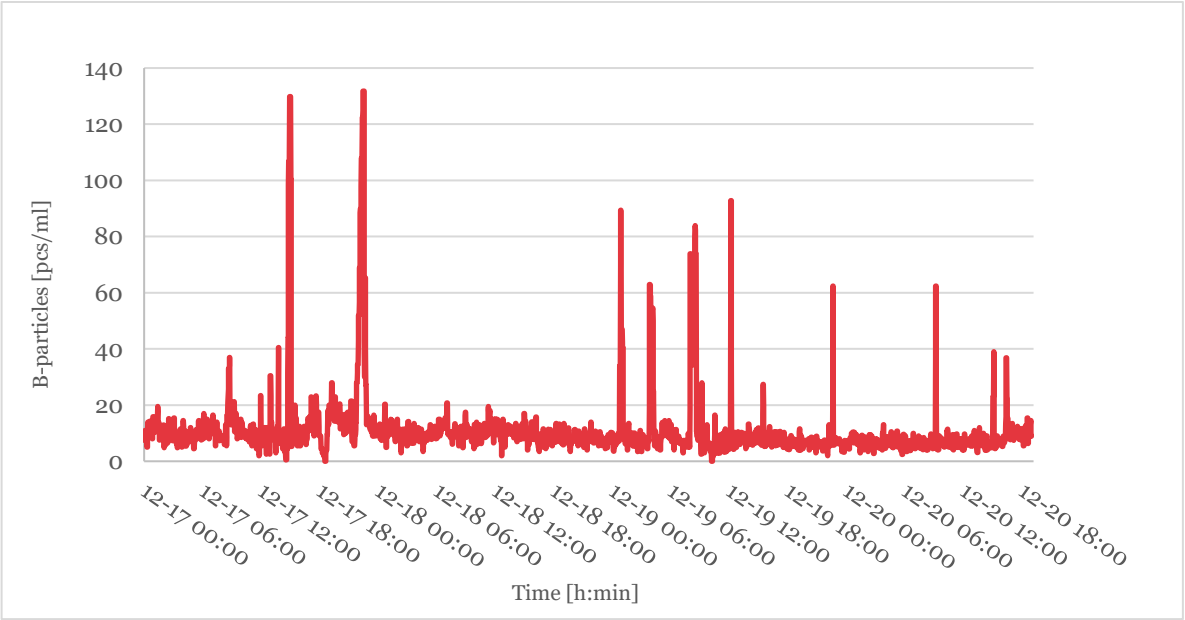

Figure 66. B-particles during event C.13.

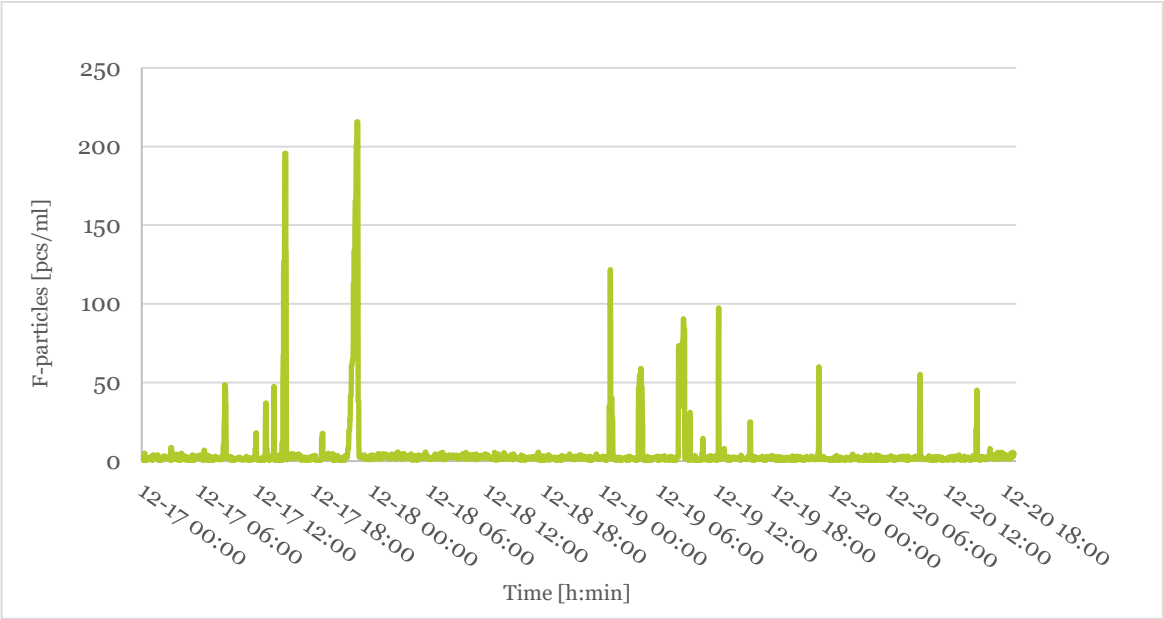

Figure 67. F-particles during event C.13.